

面向高速动态测量的光纤光栅传感信号解调技术研究进展

刘显明^{1,2*}, 任怡霖^{1,2}, 周峰^{1,2}, 雷小华^{1,2}, 章鹏^{1,2}

¹重庆大学光电技术及系统教育部重点实验室, 重庆 400044;

²重庆大学光电工程学院, 重庆 400044

摘要 以光纤光栅为传感元件的测量系统在航空航天、石油化工、国防军事等领域得到了越来越多的应用,在需要对振动冲击、动态应变等进行测量的场景中,对光纤光栅特征信号进行高速高精度解调是保障光纤光栅传感技术有效应用的关键。本文对光纤光栅高速动态信号解调方法的国内外研究现状进行了综述,按照光谱、光强、相位、微波频谱等对光纤光栅解调方法进行分类,介绍了各解调方法的原理与典型应用,对现阶段各解调方法所能实现的主要技术指标进行了分类整理。最后,对各方法的优缺点进行了对比分析,对一些涉及高速动态测量的场景以及对应可能采用的高速解调方法进行了梳理,并对高速光纤光栅解调方法的未来发展方向进行了展望。

关键词 光栅; 信号解调; 光纤传感; 高速动态测量

中图分类号 TP212 **文献标志码** A

DOI: 10.3788/CJL221313

1 引言

光纤布拉格光栅(FBG)是一种无源光器件,其本质是光纤纤芯内折射率呈周期分布的光栅^[1]。自1978年面世以来^[2],FBG已逐渐发展成为主流的光纤传感器件。与传统的电学传感器相比,FBG具有体积小、质量轻、抗电磁干扰、耐高温、串联复用等优势,在过去几十年中得到了广泛研究与应用^[3-11]。在利用FBG进行传感测量时,外界参数的变化将导致FBG光学结构参数发生变化。通过测量FBG的反射或透射光谱并进行特征分析,可以获得待测物理参量的大小。从FBG光谱信号中提取特征信息,即FBG信号解调,是进行FBG传感测量的基础。目前,基于FBG传感的系统的测量频率大多在1 kHz以下,可以满足温度、应变等参量的长期缓慢监测需求^[12];而对于振动、冲击等需高速测量的场景,基于FBG传感的方案必须满足测量速度需求才能实现有效应用。本文针对FBG在高速测量领域的应用,从解调系统方案的原理出发,根据信号采集与处理方式的不同,对FBG高速解调方法进行分类,系统地介绍了各种解调方法的工作原理、系统组成、典型应用以及发展现状,对各类FBG高速解调方法进行对比总结,对涉及高速动态测量的场景以及可能采用的高速解调方法进行了梳理,最后对FBG高

速解调的未来发展方向进行了展望。

2 FBG特征光谱及解调方法

FBG是一种波长选择器,当宽谱光经过FBG时,只有特定波长的光信号才可以被反射回去。测量FBG的反射或透射光谱,可以得到FBG的光学结构状态信息。典型的FBG反射光谱如图1所示。

反射光谱中包含很多信息,从中提取特征参数指标是高效定量分析光谱变化的有效手段^[13-20]。目前应用最多的有峰值反射率 R_{\max} 、Bragg波长 λ_B 、半峰全宽FWHM、边模抑制比SMSR这4个基本指标。其中:Bragg波长(λ_B ,单位为nm)是反射率最大时对应的波长,也被称为“峰值波长”;半峰全宽(FWHM,在公式中记为 W ,单位为nm)是光谱反射率下降到最大值一半时的宽度,可表示为 $W=W_L/2+W_R/2$, $W_L/2$ 及 $W_R/2$ 分别表示光纤光栅反射光谱的左半宽和右半宽,而且当光谱对称时, $W_L=W_R$;边模抑制比(SMSR,在公式中记为 S ,单位为dB)反映的是光谱主瓣与旁瓣的比值关系, $S=\lg(R_{\max}/R_{sl})$, R_{\max} 及 R_{sl} 分别表示光谱主瓣和旁瓣的最大值^[21]。光谱特征指标的变化可以定量反映出光谱谱形的变化。FBG信号解调可以基于不同的光谱特征指标进行。如:光谱带宽的变化可用于感知弯曲曲率^[22]和磁场^[23]的变化,边模抑制比可用于

收稿日期: 2022-10-10; 修回日期: 2022-11-23; 录用日期: 2022-11-30; 网络首发日期: 2022-12-10

基金项目: 国家自然科学基金(61875023, 51975077, 52175530)、国家科技重大专项(J2019-V-0002-0093)、重庆市自然科学基金(cstc2019jcyj-msxmX0036, cstc2020jcyj-msxmX0948)、中央高校基本科研业务费(2020CDJ-LHZZ-071)

通信作者: *xianming65@163.com

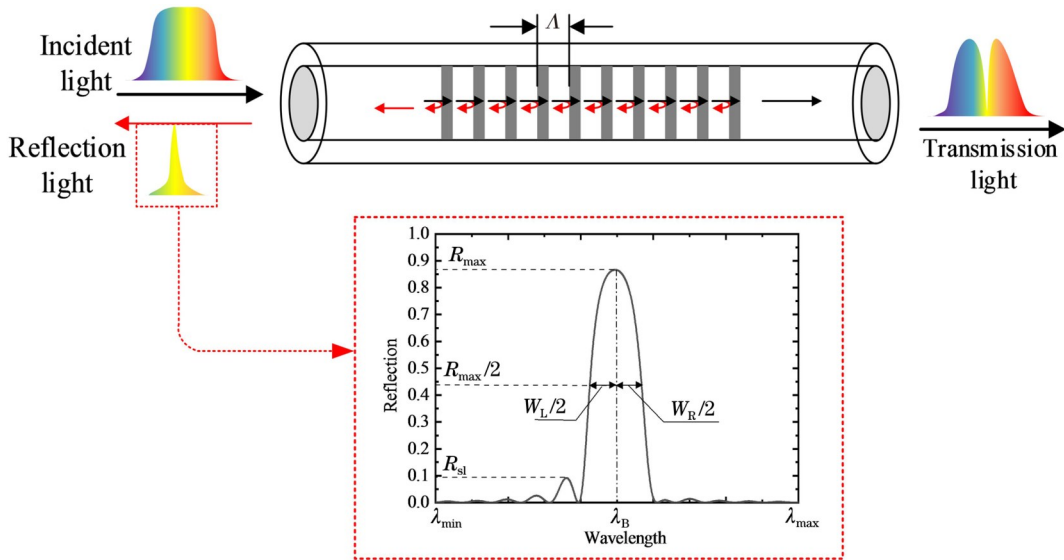


图 1 FBG 传感原理及反射光谱特征指标

Fig. 1 Fiber Bragg grating (FBG) sensing principle and reflection spectral characteristics

磁场的测量^[24],而光谱峰值波长可用于应变^[25-31]、温度^[32-35]、压力^[36-37]、湿度^[38-40]、振动^[41-42]、声学^[43-45]、磁场^[46]、电流^[47-48]、黏度^[49]等参数的测量。由此可见, Bragg 波长是高速解调中最基本的特征参数,基于 Bragg 波长变化进行信号解调也是应用最广的方式。

为高效准确地获得峰值波长信息,根据信号处理方式的不同,可将 FBG 解调方法分为三类,如图 2 所示。第一类是先获得完整的反射光谱,然后对光谱信号进行计算处理,获得峰值波长,如光谱分析法。将宽带光源与光谱仪组合,或将扫描光源与光电探测器组合,均可得到 FBG 特征光谱。第二类是通过硬件的转

换、运算将峰值波长信息转换为强度或相位信息,由此衍生出光强分析法和相位分析法。光强分析法主要采用边缘滤波的方式实现反射光谱峰值与强度的转换,典型的有单边缘滤波和双边缘滤波两种方式。相位分析法通过构造不同的干涉结构,将单束光信号转化为两束光的干涉信号,再利用干涉相位变化进行求解。根据干涉系统结构的不同可以分为非平衡马赫曾德尔干涉、迈克耳孙干涉和萨尼亚克干涉等方案。第三类是将光波域的 FBG 高频光信号与相对低频的微波进行混频,在光波域进行传感和滤波,在微波域进行信号分析,利用微波信号处理技术实现 FBG 峰值波长信息

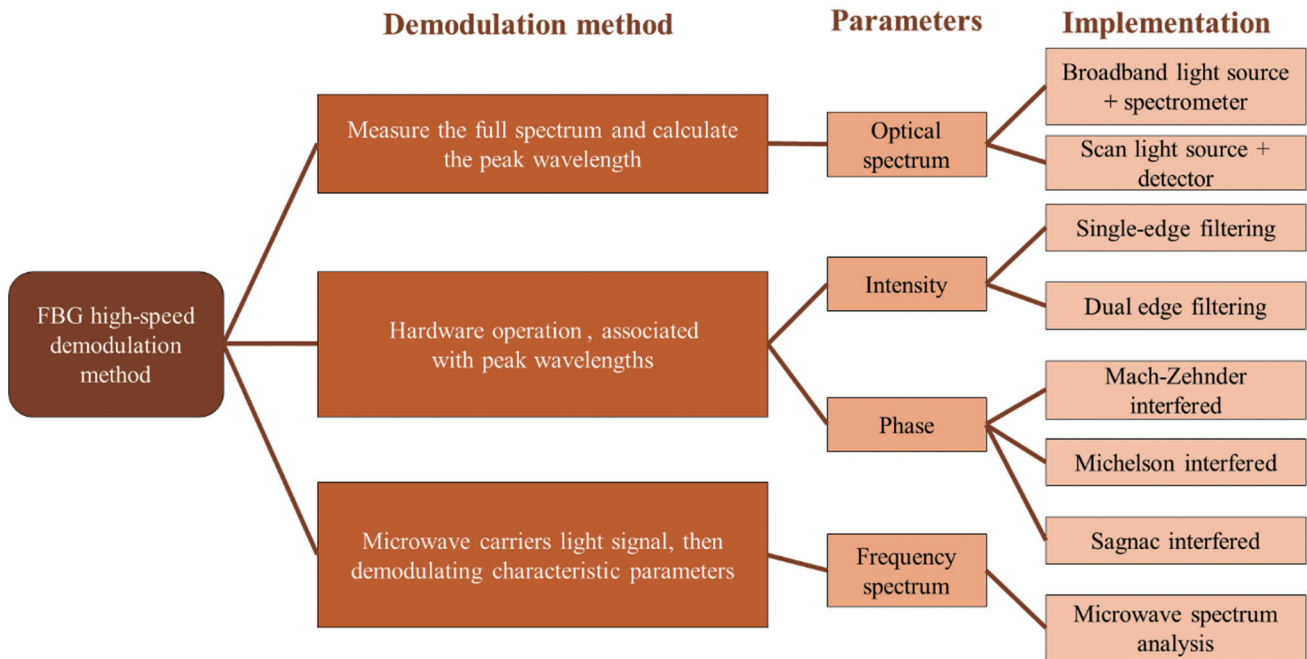


图 2 FBG 高速解调方法分类

Fig. 2 Classification of FBG high-speed demodulation methods

的提取,由此发展出微波频谱分析法。

3 光谱分析法

利用光的色散或者利用波长扫描技术,配合对应的光信号探测及处理方式,均可获得完整的反射或透射光谱,用于FBG解调。

3.1 色散式光谱测量

利用光的色散性质进行宽带光源的光谱测量是传统光谱仪的基本工作原理。基于衍射光栅、色散补偿光纤(DCF)、光子晶体光纤(PCF)、啁啾光纤光栅(CFBG)等色散元件,结合光电探测器件,均可构建光纤光谱仪。根据工作方式的不同,可将色散元件分为空间色散和时间色散两种类型。空间色散就是利用色散元件将不同波长的光在空间上分开后,由线阵探测器对光强空间分布进行探测,如图3(a)所示。时间色散就是利用色散元件使不同波长的光在时间上分散开后,通过时间域的高速测量来获得光谱信息,如图3(b)所示。

1) 空间色散

基于空间色散原理构建的FBG解调系统如图4

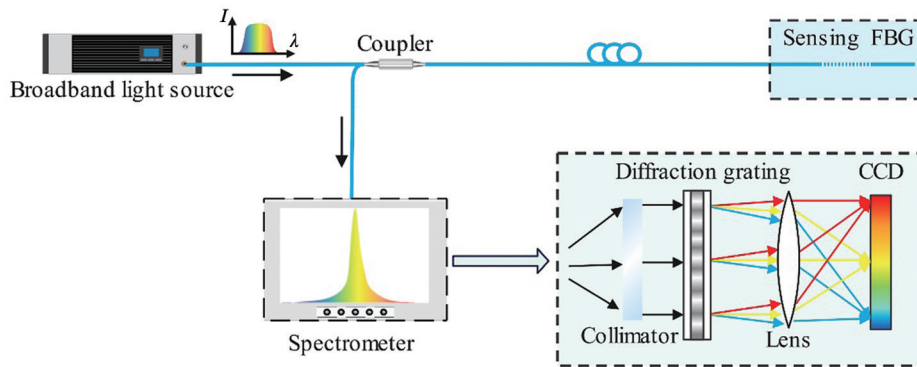


图4 空间色散法系统及原理

Fig. 4 Spatial dispersion method system and principle

2020年,Yang等^[57]利用布尼曼频率估计算法从分辨率为156 pm/unit的光谱仪中,以2 kHz的采集频率实现了0.048 pm的波长分辨率。同年,张利伟等^[58]利用Bayspec公司基于现场可编程门阵列(FPGA)制作的高速光谱仪搭配FBG对振动信号进行监测,响应频率达到了5 kHz。李佳等^[59]利用Ibsen I-MON 256商用高速解调仪对超声波导入FBG的光谱动态特性进行研究,实现了最高35 kHz的解调频率。目前,Wasatch公司生产的Cobra 1600型光谱仪的采样频率为147 kHz,Cobra-S 800型光谱仪的采样频率为250 kHz,采用速度更高的光谱仪可以进一步提高系统的测量速度。

由于线阵探测器测量速度的限制,采用空间色散方式进行光谱测量时往往需要在分辨率和解调速率两方面进行折中。提高测量速度需要以降低分辨率水平

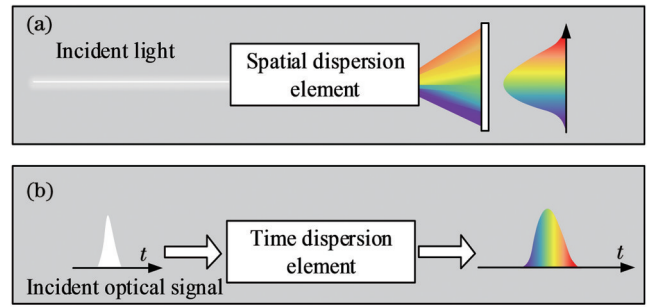


图3 FBG光谱测量的基本原理与分类。(a)空间色散;(b)时间色散

Fig. 3 Principle and classification ofFBG spectroscopy.(a)Spatial dispersion;(b)temporal dispersion

所示。光谱探测的核心元件为线阵CCD或CMOS相机,其像素密度与帧频在一定程度上决定了光谱测量的基本精度与速度。近年来,解调算法研究的深入使得在软件层面进一步提高分辨率成为可能,从而减小了分辨率对像素密度的依赖,进一步提升了光谱仪的性能^[50]。质心法^[51]、最小二乘法^[52]、最小方差移位^[53]、自相关与互相关算法^[54-55]、神经网络^[56]等方法都可以提高FBG解调的波长分辨率。

为代价,通过算法优化可在一定程度上提高波长分辨率,但核心器件FPGA的性能也会限制测量速度。

2) 时间色散

利用DCF或CFBG等色散元件使不同波长的光到达探测器的延时不同,可以实现波长-时间转换。利用高速光电探测器检测信号时延,可以获得光谱信息并将其用于解调分析^[60]。利用DCF进行FBG高速解调时,需要提供参考信号以确定时延量。利用DCF的时间色散法主要有两种实现方案:一是设置DCF和单模光纤(SMF)双光路,以SMF光路信号作为DCF光路的参考;二是在传感光路中设置基准FBG,以基准FBG作为测量FBG的参考信号。两种基于DCF的解调系统的基本结构如图5(a)和图5(b)所示。利用CFBG作为延时器件的系统的基本结构如图5(c)所示。

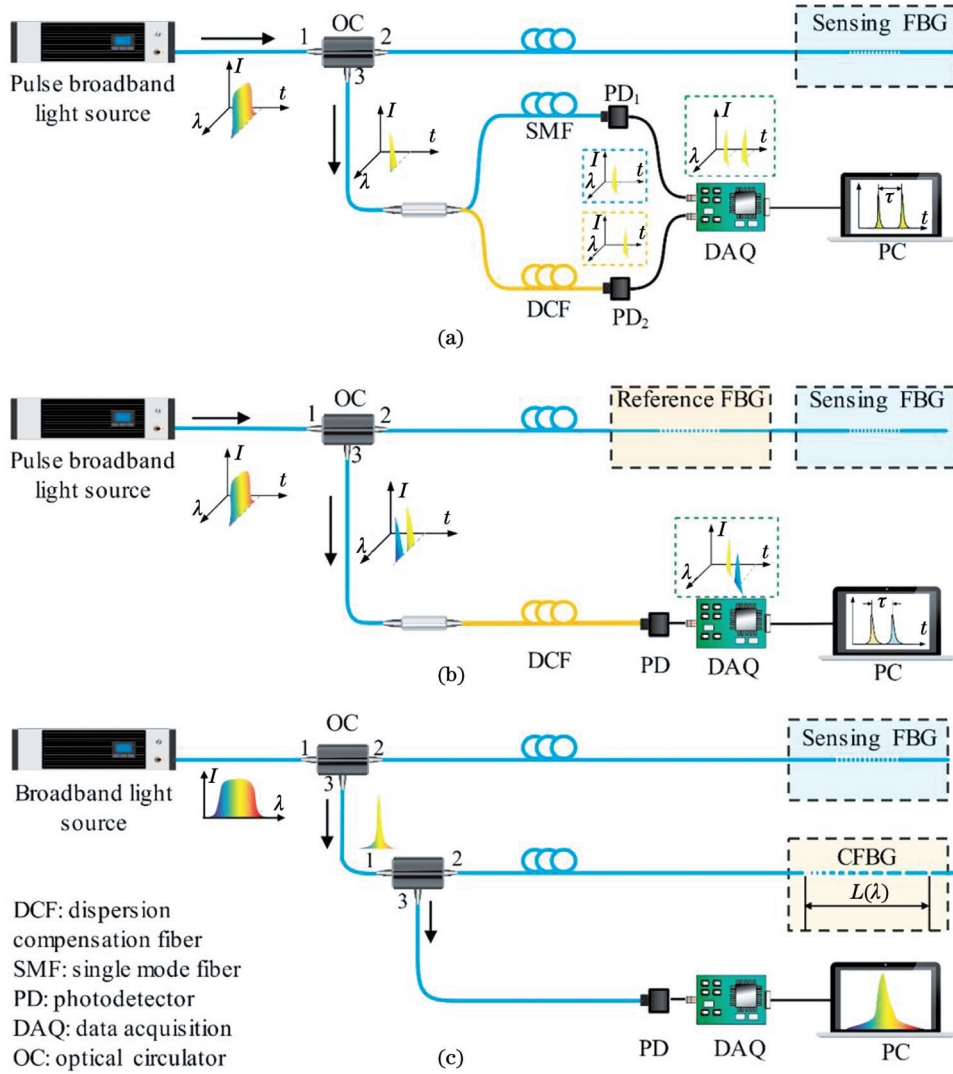


图 5 时间色散法系统及原理。(a)基于 DCF 的双光路结构;(b)基于 DCF 的双光栅结构;(c)基于 CFBG 的系统结构
Fig. 5 Time dispersion method system and principle. (a) DCF-based dual optical path structure; (b) DCF-based dual grating structure; (c) CFBG-based system structure

图 5(a)所示的双光路系统主要由脉冲宽带光源、传感链路、DCF 和 SMF、信号采集与处理模块 4 个主要部分组成。DCF 在两个脉冲之间引入可检测的波长相关延迟 τ , 这两个脉冲来自同一个 FBG, 但通过色散单元的不同臂到达。脉冲延迟 τ 的定义为

$$\tau = t_1 - t_2, \quad (1)$$

式中: t_1 和 t_2 分别是臂 1 和臂 2 的脉冲到达时间。这将光谱测量转换成了更简单的脉冲延迟测量, 避免了波长扫描。对于由同一个 FBG 反射得到的脉冲对, 脉冲延迟的变化 $\Delta\tau$ 是 FBG 峰值波长 $\Delta\lambda$ 的函数, 即

$$\Delta\tau = D \cdot L \cdot \Delta\lambda, \quad (2)$$

式中: D 为色散参数, 单位为 $\text{ps}/(\text{nm} \cdot \text{km})$; L 为色散单元的长度。在外界参数(温度、压力等)变化前后, 分别测量脉冲延迟 τ_1 和 τ_2 , 将测得的 τ_1 和 τ_2 相减即可获得 $\Delta\tau$ 。根据式(2)可得波长变化量 $\Delta\lambda$ 。

图 5(b)所示的双 FBG 系统仅含有一条传感链路, 将基准 FBG 作为参考, 将参考 FBG 与传感 FBG 间的

时间差作为脉冲延迟。图 5(c)所示解调系统以 CFBG 作为色散元件实现相位延迟。宽带光源发出的光被传感 FBG 反射, 之后通过环行器传输到 CFBG, 经历与其峰值波长成比例的相位延迟。反射光被光电探测器 (PD) 采集后送入相位检测器。在该系统中, PD 接收到的与波长相关的相位变化 $\Delta\varphi$ 与调制频率 ω_0 、光栅特性之间的关系为

$$\Delta\varphi = \frac{2L_1(\lambda)\omega_0 n}{c_0}, \quad (3)$$

式中: ω_0 为调制频率, 单位为 rad/s ; $L_1(\lambda)$ 表示 CFBG 初始位置到波长为 λ 的光被反射位置处的距离; c_0 为光在真空中的速度; n 为纤芯的有效折射率。如果光栅具有线性啁啾特性, 则其波长依赖性可以表示为

$$L_1(\lambda) = \alpha(\lambda - \lambda_0), \quad (4)$$

式中: λ_0 为传感 FBG 的 Bragg 波长; α 是由 CFBG 决定的常数。

2008年, Fu等^[61]基于DCF搭建了高速解调系统, 该系统的有效采样频率为2.44 MHz, 波长分辨率为12 pm, 可测量约37.65 nm的波长范围。2017年, Li等^[62]采用DCF对分布式FBG进行了解调, 结果显示: 设置参考FBG可以消除DCF长度扰动对系统的影响, 解调时采用动态色散值可以提高精度; 解调系统的测量频率可达1 MHz, 解调误差约为20 pm。利用CFBG进行FBG传感解调的应用也有很多^[63-67], 如: 2004年, Chtcherbakov等^[63]利用CFBG相位与波长延迟之间的依赖性进行解调, 系统的灵敏度由光栅长度和带宽决定; 2019年, Liu等^[65]利用随机光栅搭配CFBG进行波长-时间转换, 相对于数米长的光纤延时元件, 采用CFBG可在一定程度上减小延时元件的体积。

由于现有的延时元件可实现的时延量很小, 通

常需要搭配超高速信号采集系统才可以实现分光。如: G652光纤在1550 nm下的色散系数典型值为20 ps/(nm·km), 当光纤长度为10 km时, 要达到1 nm的波长分辨率, 采集频率需要达到5 GHz。而纳米级波长分辨率对于FBG光谱解调来说明显不足, 进一步提升波长分辨率对采集速度的要求更高。超高速信号采集处理系统的价格及性能限制是制约该方法速度、精度提升的主要原因。

3.2 扫描式光谱测量

利用宽带光源和可调滤波器, 或利用扫描光源和光电探测器, 均可实现FBG特征光谱的测量。宽带光源搭配可调滤波器的效果类似于可调谐激光器^[68], 滤波器可直接位于宽带光源之后, 如图6(a)所示, 也可位于传感光谱产生之后, 如图6(b)所示。

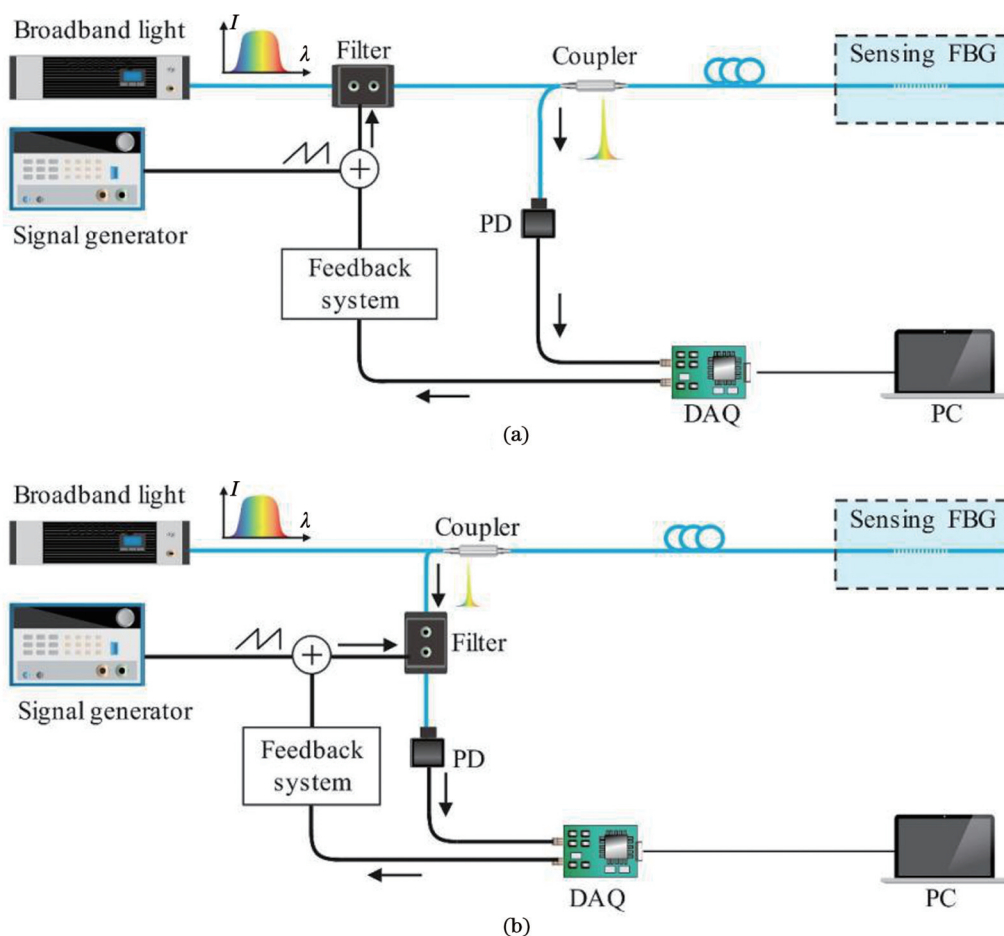


图6 基于宽带光源和可调滤波器的扫描光谱法。(a)滤波器前置;(b)滤波器后置

Fig. 6 Scanning spectroscopy based on broadband light source and tunable filter. (a) Pre-filter; (b) post-filter

当可调谐滤波器光谱与传感光栅光谱匹配时, 输出值最大, 从而可以跟踪传感光栅的波长变化^[69]。在实际应用中, 由于压电陶瓷(PZT)迟滞、蠕变和非线性等特性, 滤波器的透射波长与驱动电压难以保持良好的线性度和重复性, 高速扫描电压驱动等条件下可调谐滤波器的局部非线性特征更加明显, 而且当扫描频率增加时, 滤波器输出信噪比下降。因此, 目前系统的

扫描频率大多在5 kHz以下^[70]。如: 日本SANTEC公司的OTF-980型可调谐滤波器的调谐速度为18~25 nm/s, 加拿大WL Photonics公司的宽带可调谐滤波器的调谐速度为80 nm/s, 美国MOI公司的FFP-TF2可调谐滤波器的调谐频率为800 Hz。由于速度限制, 该方法在高速动态监测中的使用较少。

直接利用扫描光源结合高速光电探测器也可以获

得 FBG 特征光谱,典型测量系统的结构如图 7 所示。系统中的可调谐扫描光源的输出光波长随时间编码,通过周期性改变波长并进行高速同步光电探测即可得到 FBG 反射谱^[71]。系统中的关键器件是可调谐光源,根据驱动类型,可调谐光源分为电流控制驱动型光源和机械控制驱动型光源。电流控制技术通过改变注入电流实现波长调谐,具有纳秒量级的调谐速度,单输出功率较小。基于该技术的光源的典型代表是分布式布拉格反射半导体激光器(DBR)。机械控制技术基于

微机电系统(MEMS)完成波长选择,具有较高的输出功率,但扫描频率受机械结构的限制,速度水平较低。基于该技术的光源的典型代表有分布反馈式二极管激光器(DFB)、外腔激光器(ECL)、垂直腔面发射激光器(VCSEL)以及突破短腔扫描限制的傅里叶锁模激光器(FDML)等。扫描式光谱测量系统既可以用于单光纤光栅传感解调,也可以用于大容量分布式传感解调,可实现分布式传感是该系统的显著优势之一。

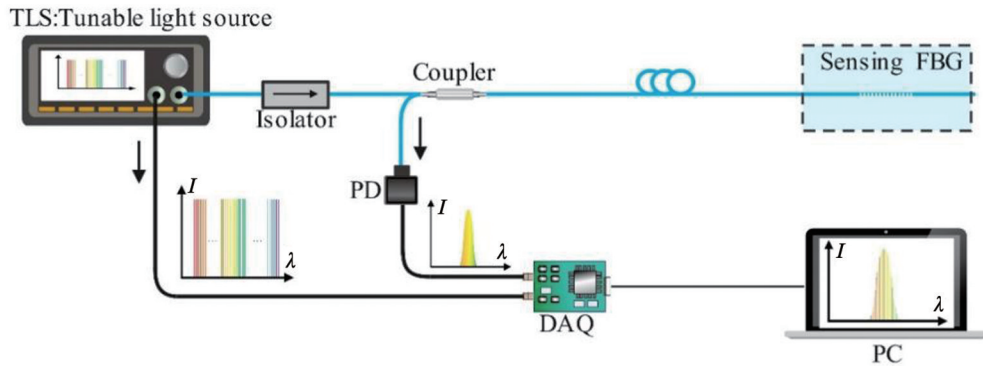


图 7 基于可调谐光源的扫描光谱法系统与原理

Fig. 7 System and principle of scanning spectroscopy based on tunable light source

DBR 采用半导体材料作为增益介质,通过改变注入电流来改变相应区域的半导体折射率,从而实现波长调节^[72]。1994年,Ball等^[73]首次采用可调谐窄带激光器以步进或连续方式输出在一定波长范围内变化的窄带光谱,对传感 FBG 进行扫描,结果发现:当特定波长的光与 FBG 峰值波长一致时,探测器探测到的光强最大;根据光强大小的变化可以重构 FBG 反射谱。2016年,郭峻^[74]采用一种新型的分布式布拉格反射半导体激光器(DS-DBR)作为可调谐光源对高频振动进行测试。他选用的 DS-DBR 的波长可调谐范围为 50 nm,波长调谐间隔为 0.4 nm,可调谐范围大,但精度和调谐速度不够高,难以满足高速 FBG 的传感需求。他将后端光栅和相位区电极作为连续可调端,并进行了一些改进,使波长连续可调谐。该 DS-DBR 的驱动电路可支持 50 nm 的光谱范围,扫描频率可达 1 MHz,系统传感精度为 0.1 pm,测量频率超过 100 kHz^[74]。

DFB 激光器是一种分布反馈式二极管激光器^[72],它在 F-P(Fabry-Pérot)激光器的基础上,将 FBG 集成到激光器内部的增益介质中。该激光器采用内部 FBG 选择工作波长,因此其谐振腔损耗具有明显的波长依赖性,这一点使得 DFB 激光器在单色性和稳定性方面优于一般的 F-P 激光器^[75]。DFB 激光器的输出波长可由驱动电流值和工作温度共同决定。2015年,武汉理工大学刘泉等^[76]利用高速调制电流驱动 DFB 激光器、光环器和光电管等器件搭建了高速 FBG 解调系统,并采用该系统对高频振动进行测试,结果表明:

DFB 激光器在 20~150 mA 驱动电流下形成了 100 kHz、1 nm 光谱范围的扫描激光器;该 FBG 解调系统可以测试 4 kHz 的振动频率,可以对振动信号进行 50 kHz 以内的频谱分析,解调精度约为 8 pm。该解调系统的解调速度很高,但波长扫描范围相对较小。2017年,该团队^[75]对上述高速 FBG 解调系统进行改进,如图 8 所示,他们结合 FBG 阵列(其波长变化小于 1 nm)使得该系统可以 100 kHz 的频率同时解调 10 个 FBG 光谱信号。结合波形缺失修复算法,该系统的动态解调范围可提高 40%。

FDML 内部设置了一段光纤延迟线,可在不牺牲扫频激光器调谐范围、瞬时线宽等参数的前提下,突破短腔谐振结构的最大扫频速度限制,从而使得波长区域的扫描频率超过 100 kHz^[77]。2008年,Jung等^[78]首次利用 FDML 扫频激光器构建的 FBG 解调系统对高速动态的振动进行测试,测量频率可达 31.3 kHz。2017年,Yamaguchi等^[79]利用扫描频率为 50.7 kHz、扫频范围为 60 nm 的 FDML 扫频光源同时对多个 FBG 进行动态传感解调,同时测量了多个频率在 kHz 量级的高速振动。2017年,该团队实现了 20 kHz 的光纤光栅解调频率,在实验平台上测量了 4.65 kHz 的高速振动^[80]。2021年,该团队^[81]进一步进行对解调系统进行改进(图 9):在光源后设置光开关和驱动,对原 FDML 的正弦波形进行剪裁,再利用缓冲级进行延迟(缓冲级有两个光路),经历不同延迟后再通过耦合器组合复用,作为测量的输入光。如此可将测量速率增加几倍。最终,在扫描频率为 50.7 kHz 的普通

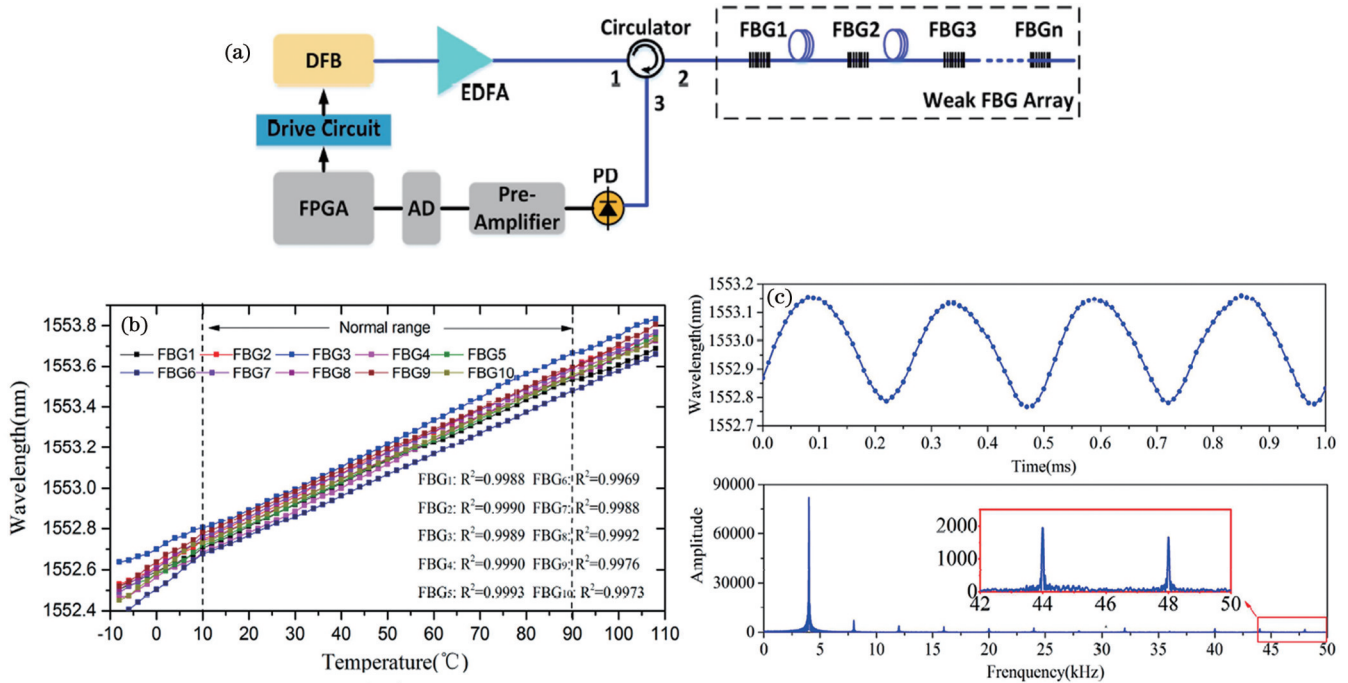


图 8 基于 DFB 光源的准分布式弱 FBG 阵列解调系统^[75]。(a) 系统结构; (b) 温度与波长之间的关系曲线; (c) 振动实验结果: 时域解调分布和频谱分布

Fig. 8 Quasi-distributed weak FBG array demodulation system based on DFB light source^[75]. (a) System structure; (b) relationship between temperature and wavelength; (c) vibration experiment results: demodulation distribution in time domain and spectrum distribution

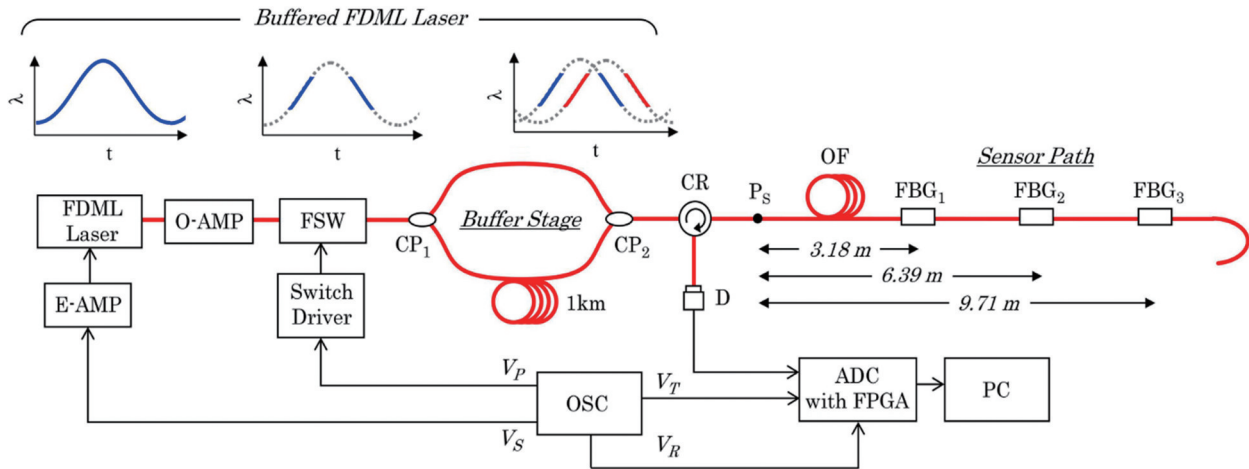


图 9 傅里叶锁模激光波长扫描法改进结构^[81]

Fig. 9 Modified structure by Fourier mode-locked laser wavelength scanning method^[81]

FDML 激光器的驱动下, 实现了 202.8 kHz 的测量频率。

综合分析上述基于光谱测量的 FBG 解调方法可知: 时间色散光谱法采用全光纤结构, 解调频率的上限最高, 且仅受脉冲光源重复频率和电学处理速度的限制, 可以达到 MHz 量级^[82]; 基于可调谐光源的扫描光谱法的 FBG 解调系统可实现 100 kHz 以上的测量频率, 在测量频率上仅次于时间色散法; 基于空间色散型的解调系统受限于线阵探测器信号的处理速度, 测量频率通常在 100 kHz 以下; 基于宽带光源和可调谐滤波器的扫描光谱法受限于高

速扫描时滤波器的非线性等特性, 测量频率通常在 1 kHz 以下。笔者总结了光谱分析法中各方案的特点以及部分典型参考文献中的性能指标, 如表 1 所示。

4 光强分析法

光强分析法将波长变化转化为强度变化, 通过硬件系统对 FBG 反射光谱进行局部强度采样(无须采集全光谱), 可大幅提高测量速度。该方法一般基于单/双边缘滤波器件实现, 如图 10 所示。

表 1 光谱法解调 FBG 的研究现状
Table 1 Research status of spectral demodulation FBG

| Demodulation method | Research institute | Year | System feature | Frequency | Resolution / pm | Range / nm |
|---------------------------------|--|------|---|-----------|-----------------|------------|
| Spatial dispersion spectroscopy | Jeonbuk National University, the Republic of Korea ^[83] | 2011 | Using diffraction grating for spectroscopy | 4 kHz | 1 | |
| | Chongqing University ^[84] | 2019 | Using dual diffraction grating for spectroscopy | 10 kHz | 63.6 | |
| | Dalian University of Technology ^[57] | 2020 | Using the Bünemann frequency estimation method | 2 kHz | 0.048 | |
| | Xi'an Technological University ^[85] | 2021 | Using a linear array InGaAs probing array with an FPGA | 17 kHz | 7 | 150 |
| Time dispersion spectroscopy | University of Ottawa, Canada ^[82] | 2011 | Using higher-order dispersion wavelength-time mapping model | 48.6 MHz | 0.61 | 20 |
| | Virginia Tech University, USA ^[86] | 2016 | Using a fast cross-correlation algorithm to calculate time delay | 20 kHz | 9.03 | |
| | Wuhan University of Technology ^[62] | 2017 | Using dynamic dispersion values | 1 MHz | | |
| | University of Valencia, Spain ^[87] | 2019 | Using an intensity Gaussian filter and dispersion to perform wavelength-time mapping | 264 MHz | 60 | |
| Scanning spectroscopy | University of Busan, the Republic of Korea ^[78] | 2008 | Using FDML laser | 31.3 kHz | 0.1 | 50 |
| | Wuhan University of Technology ^[76] | 2015 | Using DFB laser | 100 kHz | 8 | 1 |
| | Harbin Institute of Technology ^[74] | 2016 | Using self-improving DS-DBR laser and laser scanning wavelength using sinusoidal modulation | 100 kHz | 0.1 | 50 |
| | Japanese University ^[79-81] | 2021 | Using FDML laser; optical switches and MZI structures are used for cut-delay multiplexing | 202.8 kHz | | 60 |

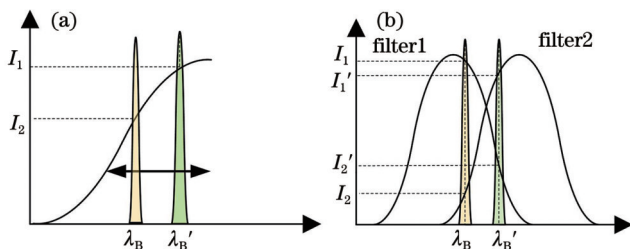


图 10 单/双边缘滤波法的原理。(a)单边缘滤波法；(b)双边缘滤波法

Fig. 10 Principle of single-/double-edge filtering method. (a) Single-edge filtering method; (b) double-edge filtering method

4.1 单边缘滤波

边缘滤波器指具有一定单值边缘的滤波器,其单值边缘一般为十几至几十纳米。FBG 反射谱的谱

宽一般为 0.2 nm,可将反射谱视为 δ 函数。当系统只存在一个滤波器时,为单边缘滤波结构,如图 11 所示。

单边缘滤波法基于输出光强与波长偏移量之间的线性关系进行解调^[88]。如图 10(a)所示,利用滤波器在一定波长范围内类线性的滤波特性,将 FBG 反射信号的峰值波长变化量转化为光强变化。光源发出的光被 FBG 反射后经耦合器分为两路,其中:一路直接被 PD 接收,作为参考来补偿强度波动;另外一路经过线性滤波器,被线性滤波器按照波长比例进行滤波。该滤波器具有与波长相关的透过率,滤波函数 $F(\lambda)$ 的线性化模型可以表示为

$$F(\lambda) = A(\lambda - \lambda_0), \quad (5)$$

式中: A 为滤波斜率; $F(\lambda)$ 在 λ_0 处等于零。

FBG 反射光谱是关于谱宽 $\Delta\lambda$ 和峰值波长 λ_b 的高

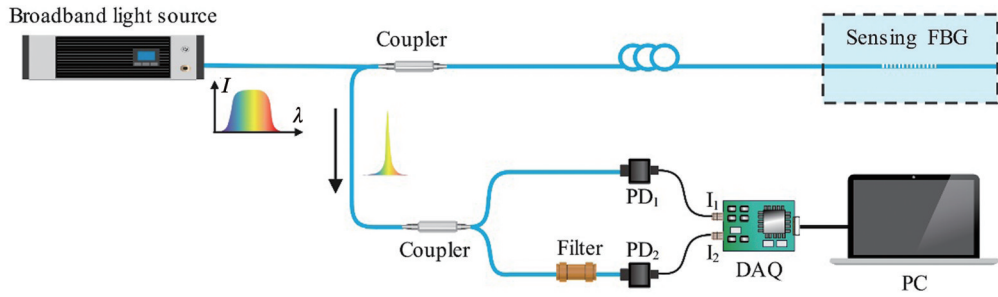


图 11 单边缘滤波法测量系统
Fig. 11 Single edge filtering measurement system

斯函数,经滤波器后的光束和参考光束的输出强度可以分别表示为

$$I_F = I_0 R A \frac{\sqrt{\pi}}{2} \left(\lambda_B - \lambda_0 + \frac{\Delta\lambda}{\sqrt{\pi}} \right) \Delta\lambda, \quad (6)$$

$$I_R = I_0 R \frac{\sqrt{\pi}}{2} \Delta\lambda, \quad (7)$$

式中: I_0 是入射到布拉格光栅上的光强; R 为光栅反射率。当输入波长改变时,参考臂的输出保持不变。两个输出的比值为

$$\frac{I_F}{I_R} = A \left(\lambda_B - \lambda_0 + \frac{\Delta\lambda}{\sqrt{\pi}} \right). \quad (8)$$

由式(8)可知,该比值会随着输入波长 λ_B 的偏移而线性变化,即: λ_B 与直接测量值 I_F/I_R 成线性关系,由此可求出 λ_B 值。

单边缘滤波法最初通过体积光学器件实现^[89],如有色玻璃带通滤波器、二色性滤波器、锥形光纤等。解调系统具有结构简单、性价比较高等特点,且不受光源

输出功率的影响,但测量精度受滤波器准直性和稳定性的影响较大,分辨率较低。为解决这些问题,研究人员提出了基于不同滤波器件的边缘滤波法,如光源滤波法和长周期光纤光栅滤波法。

光源滤波法是指利用光源光谱的类线性段进行滤波的方法。2010年,乔学光等^[90]提出了将放大自发辐射(ASE)光源的线性段作为边缘滤波器进行解调的方法。ASE光源输出的光功率密度随着波长的变化而改变,但在一定波长范围内光功率密度与波长成线性关系,而且这一关系在一定温度范围内基本不变。利用这一特点可以实现解调功能。将ASE光源的线性段作为边缘滤波器进行解调的方案省去了复杂的机械调谐部件,大大提高了系统的稳定性和扫描速度,可实现 200 kHz 的采样频率。以光源作为滤波器的线性滤波系统(图 12)的结构较为简单,扫描速度快且灵敏度很高,但光源的稳定性和质量会直接影响系统的性能,因此对光源的质量要求较高。

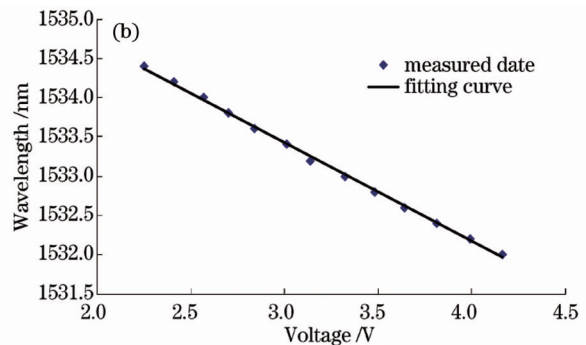
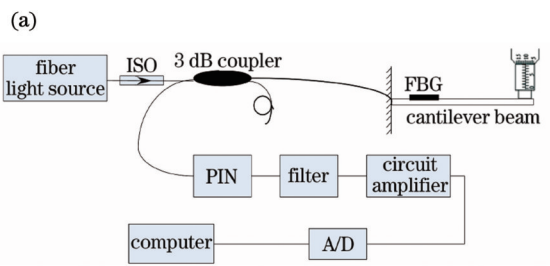


图 12 基于光源滤波的系统^[90]。(a)系统结构;(b)波长与电压的关系

Fig. 12 System based on light source filtering^[90]. (a) System structure; (b) relationship between wavelength and voltage

长周期光纤光栅(LPFG)滤波法是指利用LPFG透射谱的线性段进行滤波的方法^[91]。早在2004年,刘波等^[92]就用LPFG作为滤波器实现了数十kHz的解调频率。2016年,张燕君等^[93]将LPFG同时作为传感元件和滤波元件进行了多波长解调,如图13所示。虽然FBG的中心波长不变,但随着LPFG光谱移动,接收到的光功率发生变化,以此来实现测量。相较于体积光学和密集波分复用耦合器(DWDM),以LPFG作为

滤波器可使系统的体积有所减小,分辨率有所提高,测量范围也较大,但其缺点是对温度和弯曲敏感,需要进行温度补偿或者采用适当的封装技术才能保证测量精度。

4.2 双边缘滤波

双边缘滤波法利用两个边缘同时对FBG反射光进行滤波[图10(b)],基本的系统结构如图14所示。双边缘滤波法测量系统可以使用DWDM、F-P腔等传

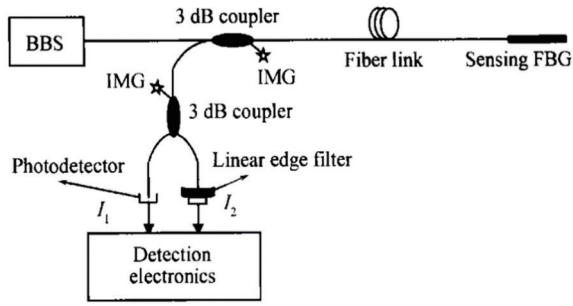


图 13 基于 LPFG 滤波的系统结构^[93]

Fig. 13 System structure based on LPFG filtering^[93]

输谱近似符合高斯函数的光学器件。两个用于滤波的

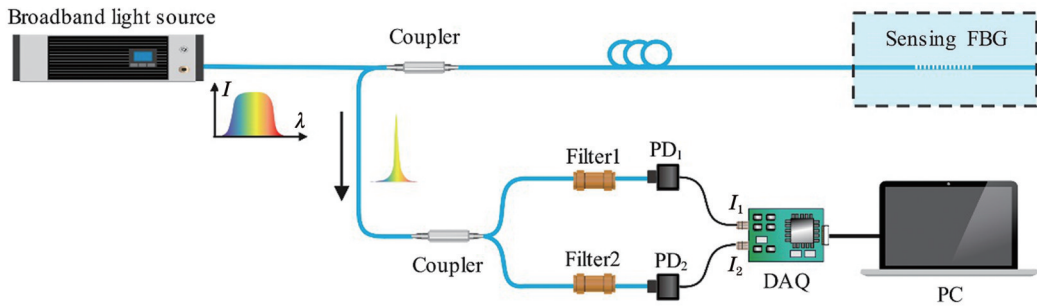


图 14 双边缘滤波法测量系统

Fig. 14 Double edge filtering measurement system

$$\rho(\lambda_i) \approx \ln(I_1/I_2) = \frac{4(\ln 2)(\Delta\lambda_{f2} - \Delta\lambda_{f1})[2x - (\lambda_{f2} - \lambda_{f1})]}{\left[\frac{\Delta\lambda_{f2} + \Delta\lambda_{f1}}{2}\right]^2 + \Delta\lambda_B^2} + \ln \frac{S(\lambda_{f2})\Delta\lambda_{f2}}{S(\lambda_{f1})\Delta\lambda_{f1}} + \frac{1}{2} \ln \frac{\Delta\lambda_{f1}^2 + \Delta\lambda_B^2}{\Delta\lambda_{f2}^2 + \Delta\lambda_B^2}, \quad (10)$$

式中： λ_{f1} 和 λ_{f2} 分别为两个边缘滤波谱的峰值波长； $\Delta\lambda_{f1}$ 和 $\Delta\lambda_{f2}$ 对应两个滤波器的半峰全宽； $S(\lambda)$ 为光源的发射谱。当 FBG 反射光谱的峰值波长满足 $\lambda_i = (\lambda_{f1} + \lambda_{f2})/2$ 时， $\rho(\lambda_i) = 0$ 。当反射谱的峰值波长移动时， $\rho(\lambda_i) \propto \lambda_i$ ，根据该线性关系可解调波长变化量。

在基于双边缘滤波的系统中，波分复用耦合器 (WDM) 两端口的透过率与反射信号波长近似成线性关系，因此 WDM 可作为滤波器使用。当反射光波长漂移时，一路光强增大，另一路光强就会减小。经过信号处理后，系统输出与反射波长成线性关系。1994 年，Davis 等^[97]将 WDM 作为滤波器，提高了系统的分辨率。边缘滤波法的波长微小漂移最终转化为强度的微小变化，波长分辨率取决于强度分辨率，更陡的线性区意味着更高的分辨率。DWDM 边缘比 WDM 更陡，因此用 DWDM 可以进一步提高分辨率和灵敏度。

阵列波导光栅 (AWG) 是实现密集波分复用光网络的理想器件，可以实现多路传感。AWG 传输谱近似为高斯函数，因此 AWG 可以作为双边缘滤波器件使用。2003 年，Sano 等^[98]提出了一种采用 AWG 的分布式 FBG 解调系统，该系统利用 AWG 相邻通道强度比值对数与 FBG 峰值波长在高斯近似下成线性关系的性质，能够以超过 0.5 pm 的精度高速检测大量 FBG

边缘相互交叠，交叠部分为测量波长的有效范围^[94]。为满足双边缘滤波的要求，两个滤波器的传输谱相交的谱宽应大于 Bragg 波长的变化范围。

FBG 反射谱函数^[95-96]可用高斯函数近似描述为

$$R_{\text{FBG}}(\lambda) = R_0 \exp\left[-4(\ln 2) \frac{(\lambda - \lambda_B)^2}{\Delta\lambda_B^2}\right], \quad (9)$$

式中： λ_B 为 FBG 的峰值波长； R_0 为反射谱的归一化系数； $\Delta\lambda_B$ 为 FBG 的半峰全宽。理论上，输出光谱等于输入光谱与其所通过信道的特征的卷积，两路 PD 探测到的光强分别为 I_1 和 I_2 。令 $\rho(\lambda)$ 为光强比值的对数，则可得

的峰值波长。2022 年，Ji 等^[99]提出并搭建了基于 AWG 的 FBG 解调仪，并对 AWG 设计中的关键参数，包括衍射级次、阵列波导数目、自由传播区长度进行了设计，在保证解调精度和分辨率的同时使测量范围扩大为原来的 4 倍。

F-P 腔具有线性范围宽和线性度好的反射/透射特性，利用 F-P 腔某一线性滤波边缘可以实现高效解调。2007 年，梁有程等^[100]提出了非对称 F-P 边缘滤波法，实现了在 7 nm 范围内的波长线性解调，测量波长分辨率为 0.01 nm。2018 年，刘睿等^[101]对现有方法进行分析和改进，提出了基于 F-P 滤波器的双边缘解调系统，该系统对滤波装置的线性特性没有严格要求。仿真分析结果显示，线性拟合的波长值与所测波长值之间的均方差为 7 pm，两者具有较好的线性度。

基于边缘滤波法的解调系统没有机械扫描部分，采用的是全光纤式解调方法，非常适用于高速动态信号的解调，测量频率可达几百 kHz^[90]。线性或类线性滤波器的线性段有限，因此需要在动态范围和测量分辨率之间进行权衡^[102]。此外，光源功率波动、光纤失调、光纤弯曲等都会导致光强不稳定，从而影响测量结果的精度和稳定性。本文总结了边缘滤波法中各方案的特点及性能指标，如表 2 所示。

表 2 边缘滤波法解调 FBG 的研究现状
Table 2 Research status of edge filtering demodulation FBG

| Demodulation method | Research institute | Year | System feature | Frequency | Resolution | Range | Sensitivity |
|-----------------------|---|------|---|---------------------------------|--------------------------|----------|---------------------------|
| Single-edge filtering | University of Bhopal, India ^[103] | 2013 | Spectrally dependent filtering of absorption in erbium-doped fibers (EDFs) is utilized | | 0.5 nm | 10 nm | 1 dB·nm ⁻¹ |
| | Yanshan University ^[93] | 2016 | Using LPFG transmission spectral as filter | 100 kHz | | 2 nm | 0.037 mV·nm ⁻¹ |
| | Hsinchu University, Japan ^[104] | 2019 | Using optical edge filter | 1 kHz (theoretical up to 5 kHz) | 0.1 pm | | |
| Dual-edge filtering | University of Skellet, UK ^[105] | 2011 | Combining active WDM and passive transient interferometry | 5 kHz | | | |
| | University of Mons, Belgium ^[106] | 2016 | Using WDM as filter | 2 kHz | 40 pm | | |
| | Xi'an University of Posts and Telecommunications ^[107] | 2018 | Using dual-core LPFG edge as filter | | 0.34439 nm ⁻¹ | 48.68 nm | |
| | University of Valencia, Spain ^[87] | 2019 | Using a picosecond laser and an active Gaussian filter | 264 MHz | 60 pm | | |
| | Beijing Jiaotong University ^[108] | 2019 | Using dense array wideband saw tooth wave (JAWS) filtering based on finite reflection virtual phase array (FRVIA) | 200 kHz | 1.22 pm | 0.89 nm | 1.1 pm·(μϵ) ⁻¹ |
| | Chongqing University of Technology ^[109] | 2021 | Using AWG and semiconductor optical amplifier (SOA) as edge filter | 120 kHz | 2 pm | 1600 pm | |
| | Beijing Jiaotong University ^[110] | 2021 | Using cross-Sagnac loop as edge filter | 200 kHz | | 3.8 nm | |

5 相位分析法

相位分析法通过干涉结构将波长解调转变为干涉条纹的相位解调,从而通过相位变化量与波长变化量之间的线性关系进行解调^[111],无须采集完整光谱。根据干涉结构的不同,相位分析法常用的干涉结构分为非平衡马赫曾德尔干涉(UMZI)结构、迈克耳孙干涉(MI)结构、萨尼亚克干涉(SI)结构。

5.1 UMZI 结构

UMZI 结构是干涉法最常用的结构之一,如图 15 所示,宽带光源输出的两束光进入两路长度相差 d 的单模光纤构成的光路(也可通过 PZT 来改变两臂相位差),再经耦合器发生干涉。

当外界环境参数发生变化,影响反射光的峰值波长 $\Delta\lambda$ 时,UMZI 两臂光信号的相位差 $\Delta\varphi$ 会发生变化,表达式为

$$\Delta\varphi = \frac{2\pi nd}{\lambda^2} \Delta\lambda, \quad (11)$$

式中 d 为两路干涉臂光路长度的差值。因此,通过检测干涉信号的相位变化可以得到峰值波长的变化。干涉法的精度较高,但测量范围相对较小。1992 年, Kersey 等^[112]首次提出了非平衡马赫曾德尔干涉法。2016 年,吴小蓉等^[113]用 2×2 和 3×3 耦合器构成 MZI 结构,成功解调了 1.5 kHz 的方波信号。理论上, MZI 结构可以解调更高频的信号。

5.2 MI 结构

MI 结构也是常用的干涉结构之一。MI 结构与 UMZI 结构类似,如图 16 所示,在两个干涉臂尾端设置反射镜,利用 PZT 控制两臂的光程差。

2001 年,余有龙等^[114]利用 MI 结构测量应变,实现了 5.5 ne 的传感分辨率。理论上,该系统具有测量动态应变的能力。2016 年,Wei 等^[115]利用反射式半导体

光放大器(RSOA)和MI结构对同一链路的多个FBG进行动态传感(图17),其中RSOA作为光源,FBG和

RSOA形成自适应光纤腔激光器。当FBG反射光谱因动态应变而发生改变时,激光输出波长就会随之发

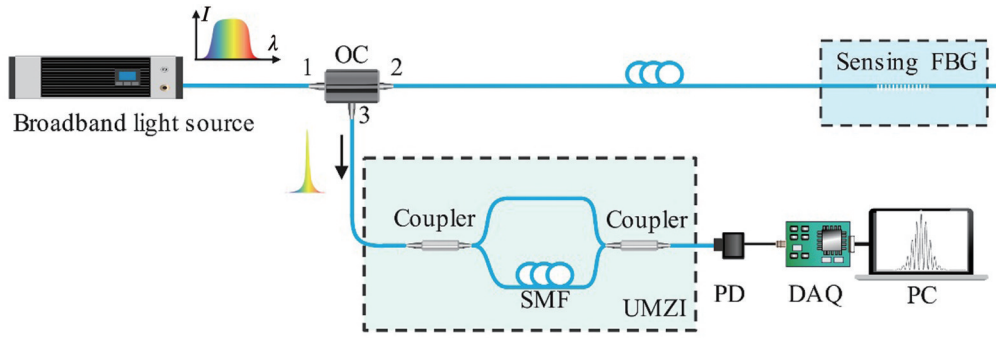


图 15 UMZI系统结构

Fig. 15 UMZI system structure

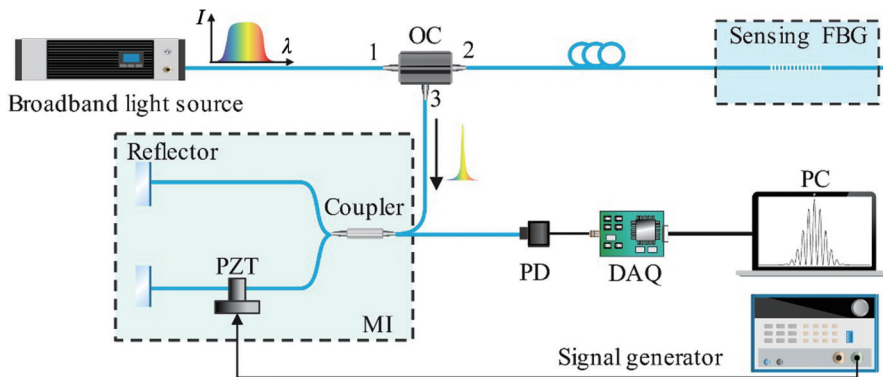


图 16 MI测量系统的结构

Fig. 16 Structure of Michelson interferometry (MI) measurement system

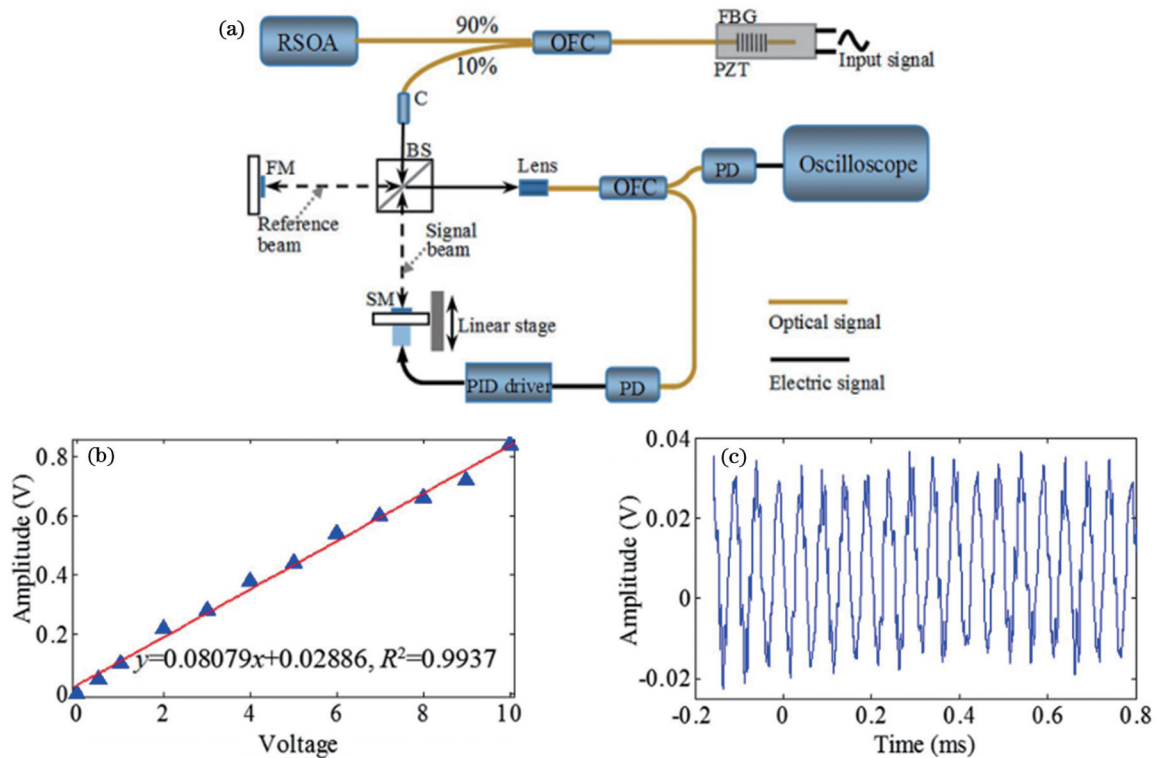


图 17 基于SOA的MI系统^[115]。(a)系统结构;(b)输出的解调幅度与施加到PZT上的电压之间的函数关系;(c)时变解调信号
Fig. 17 SOA-based MI system^[115]. (a) System architecture; (b) output demodulation amplitude is a function of voltage applied to PZT; (c) time-varying demodulation signal

生变化,将其转换为相应的相移,即可实现 20 kHz 的动态应变解调。RSOA 的过渡时间较短,因此,RSOA-FBG 腔理论上可响应 MHz 量级的高频动态应变。

5.3 SI 结构

SI 结构利用光纤萨尼亚克环路结合保偏光纤 (PMF) 构成测量系统,利用 PMF 慢轴和快轴偏振光

之间的干涉实现传播。基于 PMF 的 SI 系统的结构如图 18 所示。测量 PMF 环路镜的反射功率 I_r 和透射功率 I_t , 利用功率差 $(I_t - I_r)$ 与功率和 $(I_t + I_r)$ 的比值消除强度变化的影响。通过调整 PMF 的长度可以调整测量范围和检测灵敏度。SI 结构具有良好的偏振独立性和稳定性。

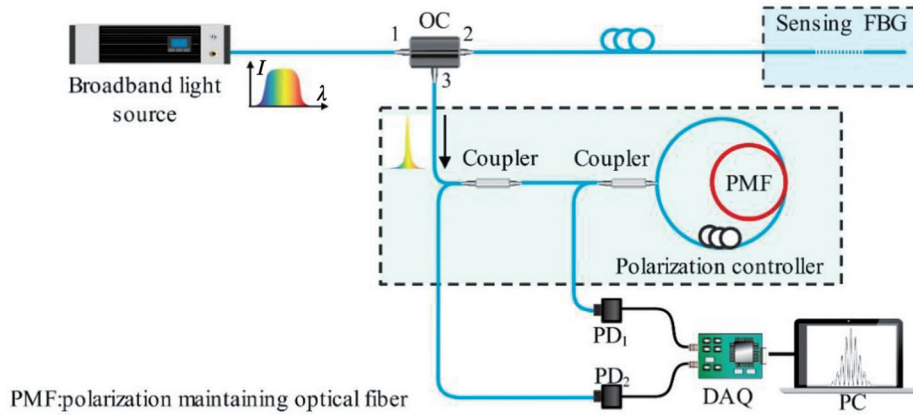


图 18 基于 PMF 的 SI 系统的结构

Fig. 18 Structure of SI system based on PMF

SI 结构由 Chung 等^[116]于 2001 年首次提出。2003 年,Zhao 等^[117]利用 CFBG 代替 PMF 构成了萨尼亚克环路,实验结果表明,该方法的动态应变分辨率为 $0.406 \mu\epsilon/\sqrt{\text{Hz}}$ 。2009 年,张锦龙等^[118]采用此方法进行温度测量,测量精度可达 $0.03 \text{ }^\circ\text{C}$,相当于 $0.3 \text{ } \mu\text{m}$ 。

2020 年,Oton 等^[119]提出利用双极化铌酸锂相位调制器构成萨尼亚克环路(图 19),其采集频率可达 100 kHz 以上,动态波长分辨率可达 $3.7 \text{ fm}/\sqrt{\text{Hz}}$,对应动态应变分辨率为 $3.1 \text{ ne}/\sqrt{\text{Hz}}$ 。

干涉法是精度很高的一种 FBG 解调方法,解调速

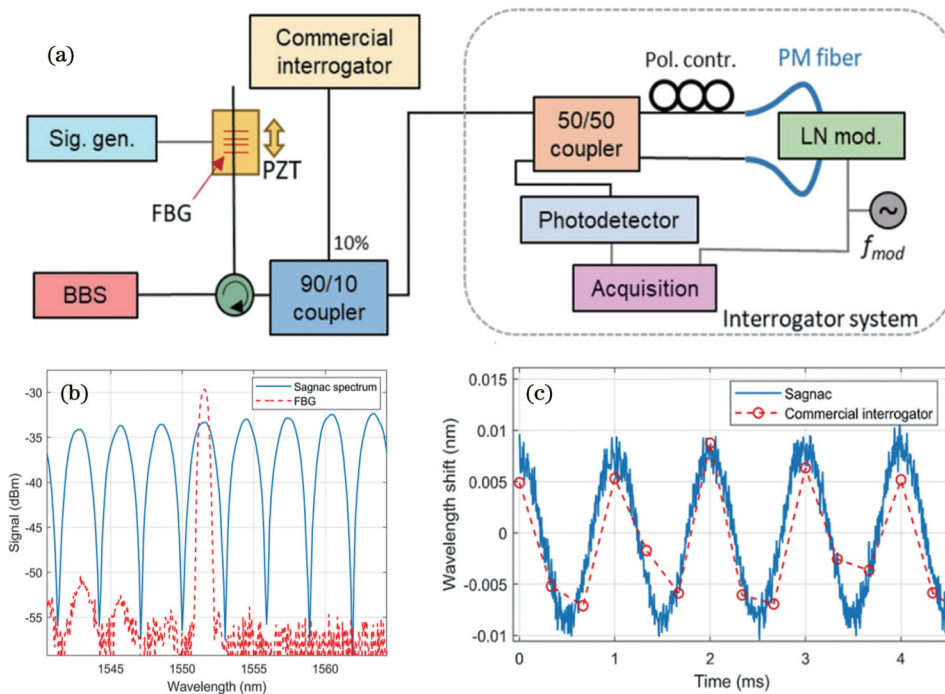


图 19 基于双极化铌酸锂相位调制器的 SI 系统^[119]。(a) 系统结构; (b) 干涉仪的透射响应光谱和 FBG 反射光谱; (c) PZT 的运动路径是频率为 10 kHz 正弦波时,该系统与商用解调仪的解调结果对比

Fig. 19 SI system based on dual-polarized lithium niobate phase modulator^[119]. (a) System structure; (b) transmission response spectrum and FBG reflection spectrum of interferometer and commercial demodulators when PZT moves in the form of a 10 kHz sine wave

度快,用于动态传感解调时,系统的动态分辨率高,可实现对高频动态信号的检测。其主要缺点是解调范围

较小。本文总结了干涉分析法中各方案的特点以及性能指标,如表 3 所示。

表 3 干涉法解调 FBG 的研究现状
Table 3 Research status of interferometric demodulation FBG

| Demodulation method | Research institute | Year | System feature | Frequency | Resolution | Range | Sensitivity |
|---------------------|---|------|---|-------------|---------------------------|-------------|---|
| UMZI | Pennsylvania State University, USA ^[120] | 2000 | Using orthogonal signal generation technology | 30 kHz | 6 nm·Hz ^{-1/2} | | |
| | Nanjing University of Science and Technology ^[113] | 2016 | MZI structure is formed with 2×2 and 3×3 couplers | 1.5 kHz | | 1177.92 με | 6.51 με·(°) ⁻¹ |
| | Indian Polytechnic University ^[121] | 2020 | Ultrasonic waves are sensed using π-FBG and interference occurs using MZI structures | | 3.7×10 ⁻³ pm | | 1.2×10 ⁸ ε ⁻¹ (theoretically) |
| MI | NASA ^[122] | 2001 | Maximize signal-to-noise ratio through time coherence analysis | >2 kHz | 0.1 nm | | |
| | Northwestern University, USA ^[115] | 2016 | Take reflective semiconductor optical amplifiers as light sources | 20 kHz | | | |
| SI | Nankai University ^[123] | 2004 | Using high birefringence polarization fibers | Tens of kHz | 0.03 °C | 7 nm | 0.092 nm·°C ⁻¹ |
| | Tianjin University ^[124] | 2019 | Output spectrum of sensor is formed by a micro-nano fiber Bragg grating (mFBG) and a Sagnac ring that measures temperature and refractive index | | | | 0.033 nm·°C ⁻¹ 39.30 nm·RIU ⁻¹ |
| | Xi'an Jiaotong University ^[125] | 2019 | Sagnac loop is formed using EDF, with FBG prepared by femtosecond laser | | | 300–1000 °C | 15.9 pm·°C ⁻¹ |
| | University of Florence, Italy ^[119] | 2020 | Using an electro-optical modulator as a tunable retarder in Sagnac loop | 100 kHz | 3.7 fm·Hz ^{-1/2} | 40 nm | |
| | Beijing Jiaotong University ^[126] | 2020 | Insert a three-segment high birefringence polarization fiber into the Sagnac ring for dual-parameter measurements | | ±0.3 °C ± 15.4 με | | -0.93 nm·°C ⁻¹ 21 pm·με ⁻¹ |

6 微波频谱分析法

FBG 是微波光子滤波器结构的一部分,在微波频谱分析法中,外界待测量通过影响 FBG 来影响 MPF 的频率响应,因此,根据频谱的变化或者频谱变化导致的输出光强变化可以解调出待测量的变化。该方法利用 MPF 实现对微波信号的采样、延时、加权等

过程。采样操作可以通过 UMZI 结构、DWDM 或 FBG 阵列实现。FBG 阵列能够通过光栅反射率控制抽头重量,通过光栅间距控制取样时间,可以实现大容量复用。如图 20 所示,在微波频谱分析法中,FBG 所处位置不同,起到的作用亦不同:1)位于光源后,进行光谱整形;2)位于电光调制器后,进行采样;3)位于光电振荡器(OEO)结构中,进行滤波。

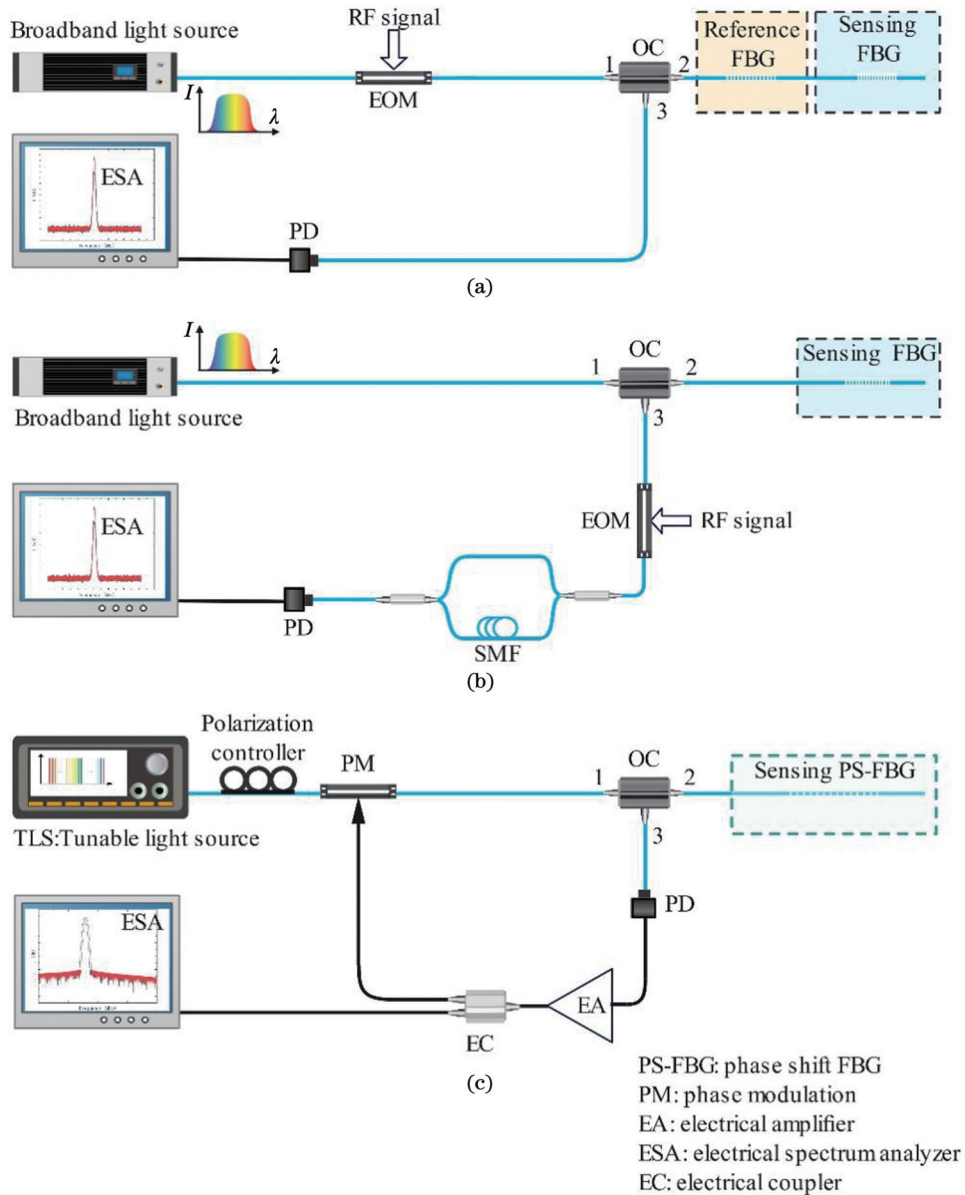


图 20 微波光子法中 FBG 的三种位置和作用。(a) FBG 位于电光调制器后,进行采样;(b) FBG 位于光源后,进行光谱整形;(c) PS-FBG 位于 OEO 结构中,进行滤波

Fig. 20 Three kinds of positions and functions of FBG in microwave photonic method. (a) FBG is located behind EOM for sampling; (b) FBG is located behind the light source for spectroscopic shaping; (c) PS-FBG is located in OEO structure for filtering

微波频谱分析法可以用于单光纤光栅的传感解调,也可以用于分布式传感网络的解调。如图 20(a)所示,当光纤光栅位于电光调制器后时,理论上可以实现分布式传感网络的解调。2008年,Dong等^[127]利用一个参考 FBG 进行温度补偿,一个传感 FBG 进行应变传感,结构如图 21 所示。当施加在传感 FBG 上的压力变化时,峰值波长就会发生变化,进而两信号之间的时延差发生改变,最终影响滤波器的频率响应。该系统实现了 $-0.34 \mu\text{V}/\mu\epsilon$ 的灵敏度,若设置多个传感光纤,就可以实现分布式光纤光栅系统的传感解调。

微波频谱分析法在单光纤光栅传感解调方面的应用更加广泛,如图 20(b)、(c)所示,当光纤光栅的作用

是光谱整形或滤波时,常常用单个光纤光栅进行传感解调。2016年,夏历课题组^[128]采用 DCF 和 SMF 作为两个干涉臂(图 22),引入差分色散,提出了微波光子法系统。在该系统中,FBG 的波长偏移可以转化为滤波器中心频率强度的变化;当环境变化时,非相干域中的干扰比相干(光学)域中的干扰更稳定。与传统 UZMI 的原理不同,该系统射频(RF)相位差转换的波长发生偏移的主要原因是两臂的差分色散。

相干光的相位对环境干扰非常敏感,环境干扰会影响解调的准确性和可靠性,而非相干域中的干扰比相干(光学)域中的干扰更稳定,所以微波频谱分析法可以有效提高系统的稳定性。此外,可以通过调节微波频率来调节灵敏度,并且可以通过使用各种低成本

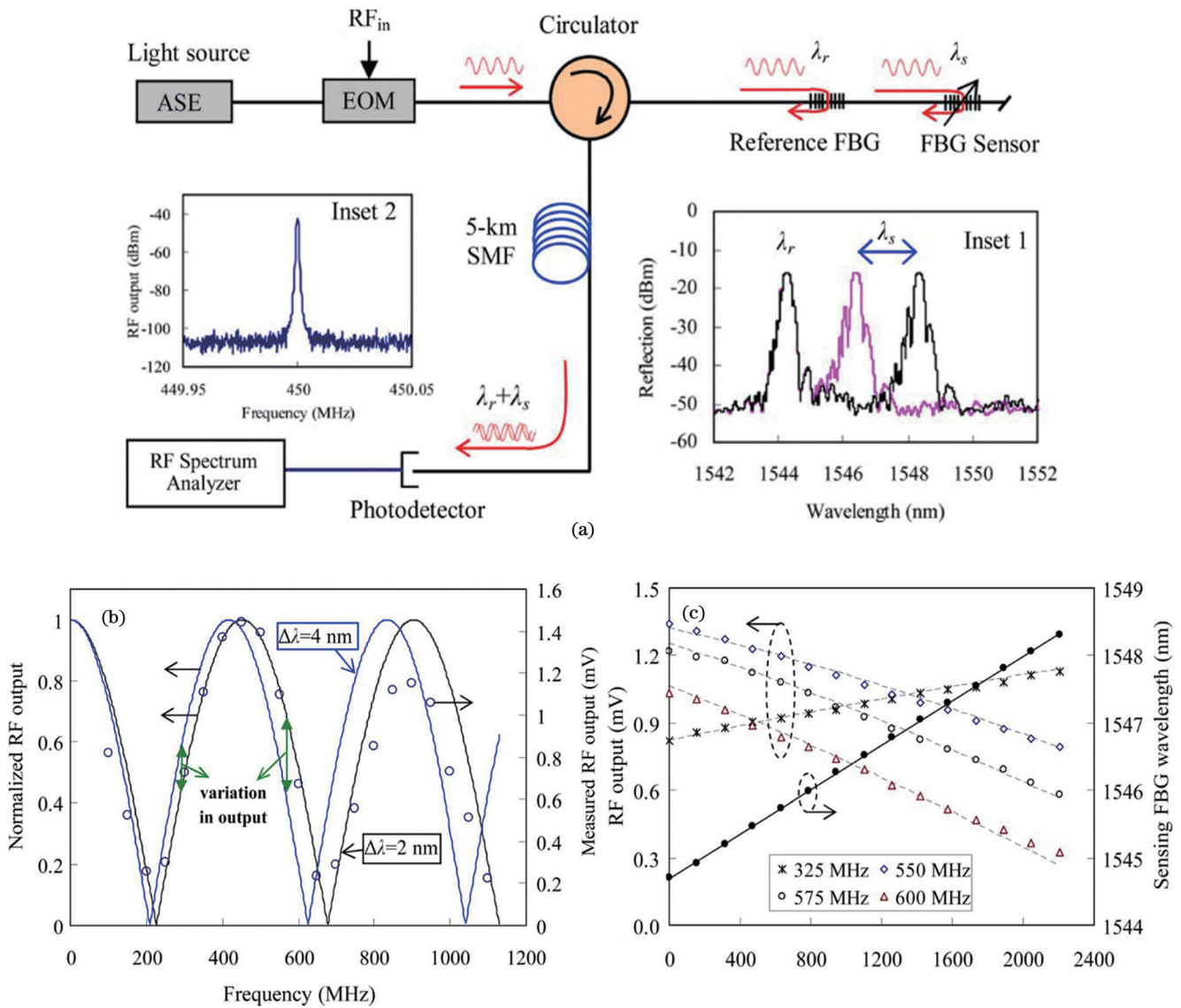


图 21 基于 FBG 的微波光子应变测量系统^[127]。(a) 系统结构；(b) 射频信号功率与调制频率的关系曲线；(c) 不同调制频率下应变测量的 FBG 波长偏移和 RF 信号功率的关系曲线

Fig. 21 FBG-based microwave photonic strain measurement system^[127]. (a) System structure; (b) relationship between RF signal power and modulation frequency; (c) relationship between FBG wavelength shift and RF signal power for strain measurement at different modulation frequencies

色散组件将灵敏度提高。

2012 年, Li 等^[129]利用光电振荡器结构实现 PS-FBG (phase shift fiber Bragg grating) 传感系统, 该系统的结构及性能如图 23 所示, 其波长分辨率可达 360 fm。2017 年, Liu 等^[130]利用微波光子法实现了对动态应力和静态应力的传感解调。为进一步提高测量速度, 2018 年, Zhou 等^[131]采用交叉扫描周期来形成拍频, 使得测量频率达到 40 kHz。

微波光子法利用电光调制器将微波调制至光载波上, 使信号在光纤中传输(减小损耗), 同时利用成熟的电子技术完成对信号的操作, 发挥微波与光纤通信技术各自的长处, 降低系统的实际操作成本, 并提高测量速度和传感精度。本文总结了微波频谱分析法中各方案的特点以及性能指标, 如表 4 所示。

7 现状总结与应用需求分析

将前文各方法的典型参数及解调原理进行分析后, 可总结出各方法的主要优缺点、适应场景以及能否进行多光栅测量等, 如表 5 所示。

在上述高速解调方法中, 部分方法已形成了商业化产品, 但大部分还停留在实验室探索阶段。空间色散的全光谱测量与解调方法发展得较为成熟, 目前已有许多商业化的高速光谱仪可供选择, 其频率可高达上百 kHz。结合宽带光源形成的解调系统是相对简单且成熟度较高的系统。基于时间色散光谱的解调方法需要搭配高速数据采集模块(采样频率通常要求达到 GHz 以上), 目前虽然已有基于时间色散原理的光谱仪产品, 但选择较少, 更多系统仍停留在实验室

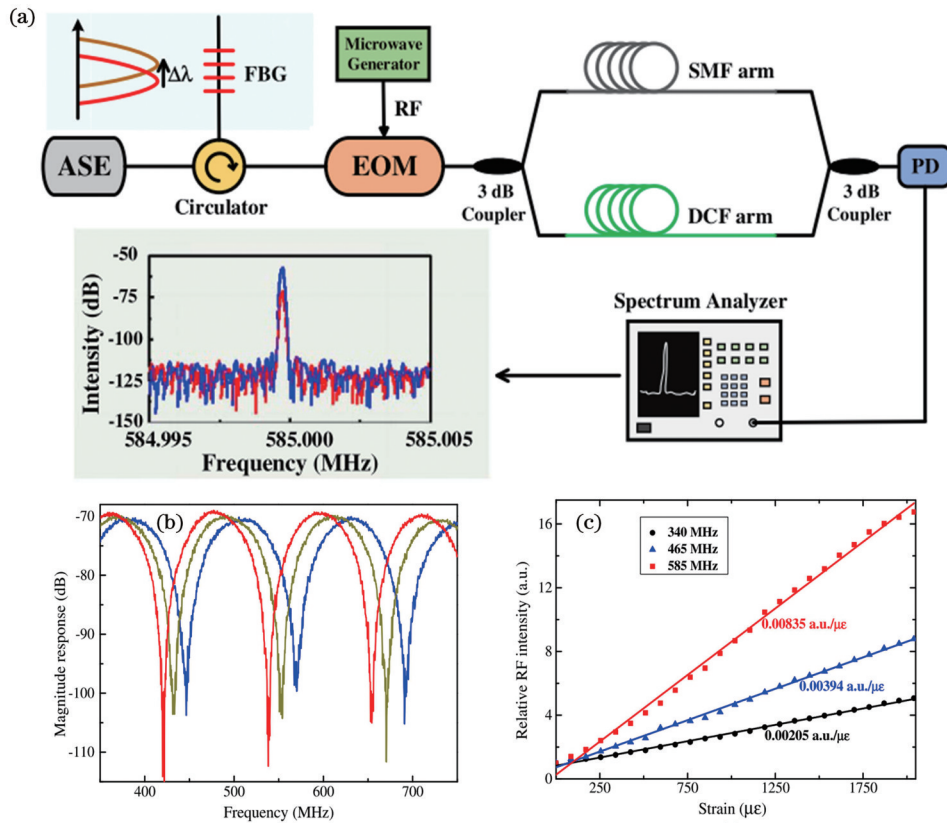


图 22 微波光子法系统^[128]。(a)系统结构；(b)在FBG上施加不同应变时的微波干涉光谱；(c)不同调制频率下应变与相对RF强度的关系

Fig. 22 Microwave photonic method system^[128]. (a) System structure; (b) microwave interference spectra when different strains are applied to FBG; (c) relationship between strain and relative RF intensity at different modulation frequencies

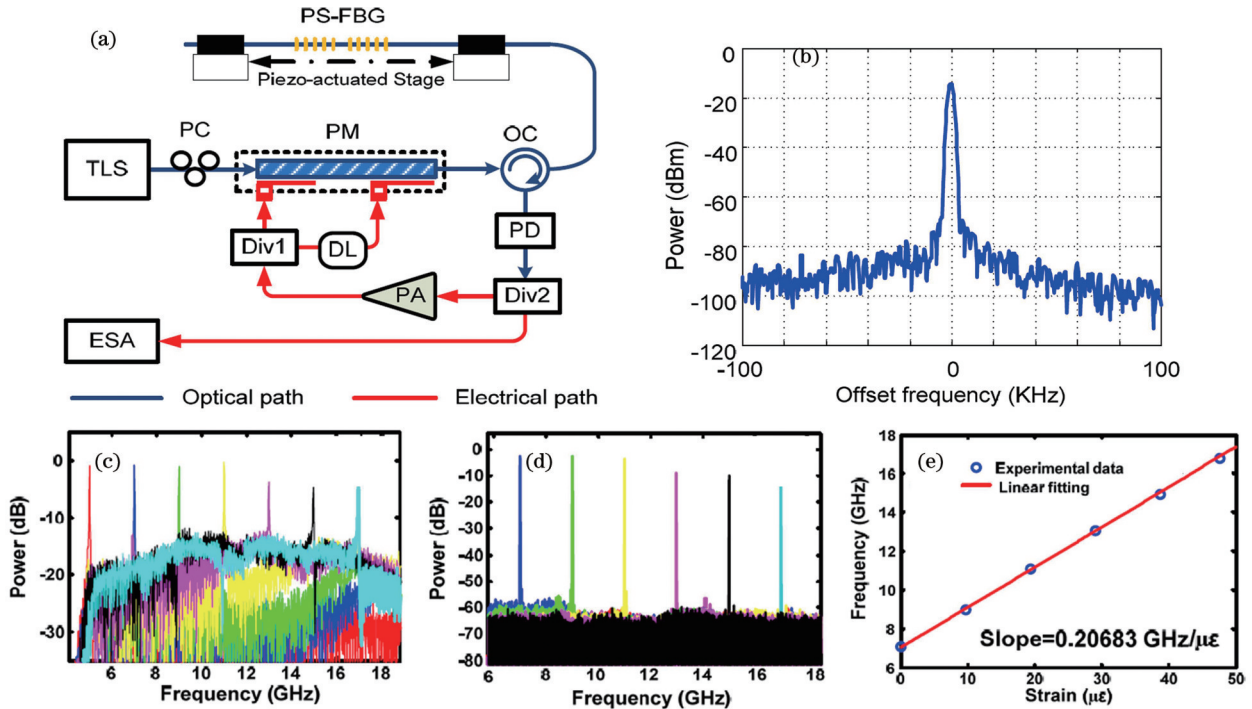


图 23 PS-FBG 传感系统^[129]。(a)系统结构图；(b)OEO 环路生成的微波信号的光谱；(c)不同应变下的频率响应；(d)不同应变下 OEO 输出端产生的微波谱；(e)施加的应变与产生的微波信号的频率之间的关系

Fig. 23 Phase shift fiber Bragg grating (PS-FBG) sensing system^[129]. (a) System structure diagram; (b) spectrum of microwave signal generated from OEO loop; (c) frequency response for different applied strains; (d) spectra of generated microwave signal at OEO output for different strains; (e) relationship between applied strain and the frequency of generated microwave signal

表 4 微波光子法解调 FBG 的研究现状

Table 4 Research status of FBG demodulation by microwave photonic method

| Research institute | Year | System feature | Frequency | Resolution | Range | Sensitivity |
|--|------|--|-------------------|-------------------|--|--|
| University of Ottawa, Canada ^[132-133] | 2015 | Using PS-FBG to form a tunable OEO | MHz | | | $9.73 \text{ GHz} \cdot \text{N}^{-1} \cdot \text{mm}$ |
| Polytechnic University of Valencia, Spain ^[134] | 2015 | Cascading 7 FBGs for spectral sampling | | 14 pm | | |
| Huazhong University of Science and Technology ^[128] | 2016 | Differential dispersion is introduced using MZI structures | | 0.01 dB | | $0.85 \text{ arb. units} \cdot \mu\epsilon^{-1}$ |
| ITEAM Institute, Spain ^[135] | 2017 | Combining low-coherence interference techniques with MWP | A few hundred MHz | | | $2.47 \text{ GHz} \cdot \text{mm}^{-1}$ |
| Nanjing Normal University ^[136] | 2018 | Sampling is performed using bias-preservative fibers | | 0.01 N | | $9.87 \text{ MHz} \cdot \text{N}^{-1}$ |
| Wuhan University of Technology ^[131] | 2018 | Using phase modulation and cross-scan cycles to form the beat frequency | 40 kHz | | | |
| University of Sydney, Australia ^[137] | 2019 | Combining low coherence interference technology and dispersion media | | 124 μm | | $5.56 \text{ GHz} \cdot \text{mm}^{-1}$ |
| Nanjing University ^[138] | 2020 | Based on wavelength-to-fiber relative delay (OFRD) mapping | | 2 pm | $> 300 \text{ }^\circ\text{C}$ ($> 3 \text{ nm}$) | |
| Nanjing University ^[139] | 2020 | Cascading raster arrays are connected to the OEO oscillation loop via a circulator | | | 2 kHz | $1.3 \mu\epsilon \cdot \text{pm}^{-1}$ $0.1 \text{ }^\circ\text{C} \cdot \text{pm}^{-1}$ |
| Nanjing University ^[140] | 2020 | Based on WTT mapping and multi-ring OEO | | 20 pm | $619.04 \mu\epsilon$ (24.7 kHz) | $40.2 \text{ Hz} \cdot \mu\epsilon^{-1}$ $146.5 \text{ Hz} \cdot \text{ }^\circ\text{C}^{-1}$ |
| Xiamen University ^[141] | 2022 | Using cursor effect and bicyclic OEO to improve sensitivity | | 1–1000 Hz | | $141.13 \text{ kHz} \cdot \text{ }^\circ\text{C}^{-1}$ |

表 5 各解调方法的优缺点

Table 5 Advantages and disadvantages of each demodulation method

| Method | Principle | Advantage | Disadvantage | Demodulation applicability | Number of FBG sensor |
|-------------------|---------------------------------|---|---|---|-------------------------|
| | Spatial dispersion spectroscopy | High precision and reliability | Speed is relatively slow | High-precision measurement scenarios that require relatively low speed | Single or multiple FBGs |
| Spectral analysis | Time dispersion spectroscopy | Extremely fast and extremely high ceiling | 1) Low accuracy 2) Requirements for signal acquisition speed are extremely high | Scenes where the measured quantities change very quickly and the measurement accuracy is not required | Single FBG |
| | Scanning spectroscopy | High signal-to-noise ratio and resolution | 1) Speed is limited by mechanical drive 2) Affected by stability of light source 3) Speed is increased to a certain degree. Linearity of light source decreases | Scenes that require high accuracy and resolution | Single or multiple FBGs |

(续表)

| Method | Principle | Advantage | Disadvantage | Demodulation applicability | Number of FBG sensor |
|-----------------------------|---------------------------|---|--|--|-------------------------|
| Intensity analysis | Edge filtering method | All-fiber structure, high speed | 1) Fluctuation of power of light source itself 2) There is a linear approximation of the filter curve | Scenes that require low accuracy and require real-time dynamic demodulation | Single FBG |
| Phase analysis | Interference method | High accuracy and resolution | Demodulation range is relatively small | Scenes where the range of change to be measured is not large | Single FBG |
| Microwave spectrum analysis | Microwave photonic method | Improved stability, extremely high resolution and sensitivity | System structure is relatively complex | Special scenarios such as high system stability requirements and multi-mode transmission | Single or multiple FBGs |

研究阶段。扫描式光谱分析系统在速度、精度、分辨率上的表现较为均衡,在多光栅串联的准分布式传感测量领域的应用潜力较大。目前一些高速光源模块产品的频率可达 MHz 以上,结合高速探测器即可完成解调系统的搭建,是精度、速度较为均衡的实用化系统。光强法解调系统是无机械结构,也是测量速度最高的系统,但其对传感器、解调系统的稳定性要求极高,仅能在测量精度要求较低的场景中应用。此外,由于不能获得完整的光栅光谱,光强法解调系统必须根据光纤光栅传感器的特征光谱进行波长选择和系统定制,存在通用性不足的问题,难以形成通用产品。相位分析法解调系统的测量精度高,但测量范围较小,与光强法解调系统一样存在定制化问题,在实际应用中存在较大局限性。在众多方法中,微波频谱分析法的灵敏度表现较为突出,具有极高的灵敏度和分辨率,系统搭建灵活度高,还可用于多光栅解调,是近几年高速发展的一类解调方法,但目前仍处于实验室探索阶段,尚未形成商业化产品。未来若在某一方向进行针对性研发,很有可能形成性价比比较高的解调系统。

高速动态测量的实际应用场景非常多,所需达到的测量频率各不相同。如:航空齿轮箱内齿轮的啮合频率可达 8.2 kHz^[142],叶片发生的高阶共振频率可达 11.1 kHz^[143],对应的基于 FBG 的应变/振动等测量系统的频率须达到 10 kHz 量级。在研究炸弹爆炸形成的冲击波的各项参数时,解调系统的测量频率必须大于冲击波的瞬时频率,要求解调频率为 100 kHz 甚至更高^[144],才能实现有效测量。因此,高速 FBG 解调系统的研究与开发对于满足高速动态信号日益增长的实时解调监测需求具有重要意义,而且具有很高的实用价值和广阔的市场前景^[145-149]。图 24 列出了一些典型的高速 FBG 解调需求场景以及对应的可能采用的解调方法。

由前文分析可知,每一种解调方法都有自己的优

势和不足,实际应用时需根据精度、速度、量程、稳定性以及价格等需求进行选择。比如对于桥梁、铁轨等大型结构振动及动态应变的测量,应用环境相对稳定,对测量速度和量程的要求可能相对较低,利用分布式传感进行多点监测可以提高效率和性价比。由于长期使用,对测量精度、系统稳定性、数据输出实时性的要求较高,扫描式光谱测量方法或者微波频谱分析法都是比较好的选择。而对于爆炸冲击波的冲击威力和目标载荷响应的瞬时监测,分布式传感反而会降低系统的可靠性,单点且高速的采集方法会更加适用。此类瞬态测量对速度、量程要求较高,但测量时间短,可先采集后处理。由于实际测试时往往需要监测多点,对于单点测量所对应的系统单价要求不能太高,此时利用基于边缘滤波的光强分析法进行测量是相对合适的选择。总之,应用环境和测量需求是多样性的,根据不同场景选择不同的高速解调系统和方法,充分发挥各类解调方法的独特优势,是实现高效精准测量的基本前提。

8 结束语

根据上述 FBG 解调技术的研究现状及应用需求,未来 FBG 解调技术可能的重点发展方向包括以下几方面:

1) 提高系统的解调速度。FBG 测量系统的解调速度由两部分决定,分别是特征信号采集探测速度以及信号分析处理速度,本文主要对 FBG 特征信号的高速采集获取方式进行了综述。目前,点式光电探测器的带宽、高速数据采集频率都可达数十 GHz,限制 FBG 信号探测速度的主要因素有光源、调制器的调制速率、线阵探测器的帧率、数据采集能力等。未来可通过提升这些器件的速率来进一步提高解调系统对 FBG 信号的高速探测能力。此外,对于一些需要实时解调的应用场景,如航空发动机脉动压力的测量现场等,在保证一定精度的前提下有效提高信号分析处理

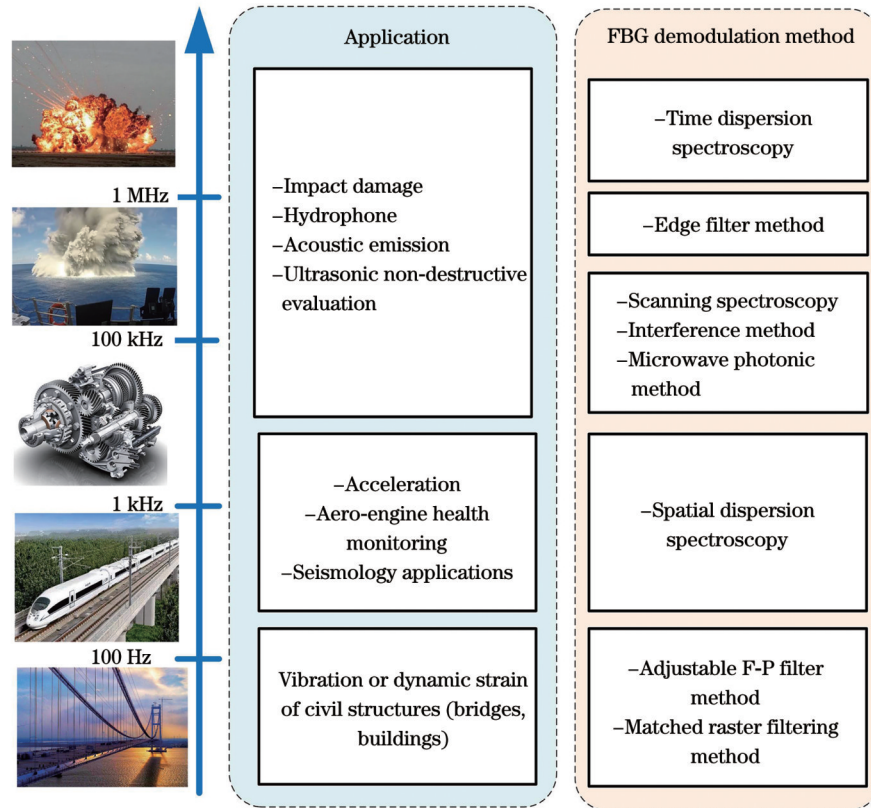


图 24 高速 FBG 解调需求与方法

Fig. 24 High-speed FBG demodulation requirements and methods

的速度,是实现高速实时解调的关键。因此,当信号的采集、探测速度提升后,后端信号的分析处理能力将成为制约系统解调速度的瓶颈。在保证解调精度的同时优化解调算法,提升计算速度,也是未来提高实时解调速度的重要发展方向。

2) 提高系统的解调精度。在 FBG 解调系统中,光源的光谱范围和分辨率在很大程度上决定了系统的测量范围和精度。高速解调系统的常用光源包括宽带光源、脉冲光源及扫频光源,选择高性能光源是提高系统精度的基础。获得更高的扫频速度和输出功率,实现线性光谱输出以及获得稳定的相位,是光源未来的发展方向。此外,采用边缘滤波法时,滤波器的稳定性和线性度也会影响系统的精度。系统越复杂,误差来源就会越多。提高系统精度必须保证系统中关键器件的性能、质量,也可通过增加参考的方式消除部分误差,提高精度。

3) 提高系统的解调容量。光纤光栅传感的一大优势是能实现多光栅串联的准分布式测量。表 5 中所列方法并非都能实现多光栅的解调,边缘滤波法、干涉法等主要在单光栅解调中应用。要实现多点分布式测量,需要获得大范围的光谱或频谱数据。在提升光谱测量速度的同时进一步扩展光谱带宽,是准分布式大容量光纤光栅高速解调技术发展及应用的基础。此外,微波光子结合啁啾光栅的方法在实现高速大容量分布式传感方面也具有一定潜力。

参 考 文 献

- [1] 饶云江, 王义平, 朱涛. 光纤光栅原理及应用[M]. 北京: 科学出版社, 2006.
Rao Y J, Wang Y P, Zhu T. Principle and application of fiber grating[M]. Beijing: Science Press, 2006.
- [2] Hill K O, Fujii Y, Johnson D C, et al. Photosensitivity in optical fiber waveguides: application to reflection filter fabrication[J]. Applied Physics Letters, 1978, 32(10): 647-649.
- [3] Jiang J F, Yang Y N, Zhang X Z, et al. Distortion-tolerated high-speed FBG demodulation method using temporal response of high-gain photodetector[J]. Optical Fiber Technology, 2018, 45: 399-404.
- [4] 刘铁根, 王双, 江俊峰, 等. 航空航天光纤传感技术研究进展[J]. 仪器仪表学报, 2014, 35(8): 1681-1692.
Liu T G, Wang S, Jiang J F, et al. Advances in optical fiber sensing technology for aviation and aerospace application[J]. Chinese Journal of Scientific Instrument, 2014, 35(8): 1681-1692.
- [5] Li C, Sun L, Xu Z Q, et al. Experimental investigation and error analysis of high precision FBG displacement sensor for structural health monitoring[J]. International Journal of Structural Stability and Dynamics, 2020, 20(6): 2040011.
- [6] Hu Y H, Wan S P, Shi J L, et al. Research on high resolution fiber Bragg grating sensing technology based on high speed parallel sampling[J]. Optics Communications, 2019, 435: 126-128.
- [7] Sun X Y, Zeng L, Hu Y W, et al. Fabrication and sensing application of phase shifted Bragg grating sensors[J]. Materials, 2022, 15(10): 3720.
- [8] Li C L, Tang J G, Cheng C, et al. FBG arrays for quasi-distributed sensing: a review[J]. Photonic Sensors, 2021, 11(1): 91-108.
- [9] Bonopera M. Fiber-Bragg-grating-based displacement sensors: review of recent advances[J]. Materials, 2022, 15(16): 5561.

- [10] 孙世政, 刘照伟, 张辉, 等. 基于 HHO-KELM 的 FBG 流量温度复合传感解耦[J]. 光学精密工程, 2022, 30(11): 1290-1300.
Sun S Z, Liu Z W, Zhang H, et al. Decoupling of FBG flow and temperature composite sensing based on HHO-KELM[J]. Optics and Precision Engineering, 2022, 30(11): 1290-1300.
- [11] 刘芳芳, 杨子涵, 焦宇辉, 等. 皮米量级微位移信号处理分辨率的光纤布拉格光栅探针系统[J]. 光学精密工程, 2022, 30(7): 755-764.
Liu F F, Yang Z H, Jiao Y H, et al. Fiber Bragg grating probe system with picometer-level micro-displacement signal processing resolution[J]. Optics and Precision Engineering, 2022, 30(7): 755-764.
- [12] 张鼎博, 李俊, 张维, 等. 光纤光栅传感技术在异形结构健康监测中的应用[J]. 激光与光电子学进展, 2022, 59(5): 0505001.
Zhang D B, Li J, Zhang W, et al. Application of fiber Bragg grating sensing technology in the health monitoring of special-shaped structures[J]. Laser & Optoelectronics Progress, 2022, 59(5): 0505001.
- [13] Wang T L, Li Y, Tao J C, et al. Deep-learning-assisted fiber Bragg grating interrogation by random speckles[J]. Optics Letters, 2021, 46(22): 5711-5714.
- [14] Zhao B Y, Li W, Xia L, et al. Multivision demodulation of the FBG based on a thermal-induced chirp and a shallow neural network[J]. Applied Optics, 2021, 60(22): 6503-6510.
- [15] Wu N S, Xia L. Interrogation technology for quasi-distributed optical fiber sensing systems based on microwave photonics[J]. Chinese Optics, 2021, 14(2): 245-263.
- [16] Wu H, Lin Q J, Han F, et al. Design and analysis of high-frequency fiber Bragg grating vibration sensor[J]. Measurement Science and Technology, 2021, 32(2): 025108.
- [17] Yu X K, Song N F, Song J M. A novel method for simultaneous measurement of temperature and strain based on EFPI/FBG[J]. Optics Communications, 2020, 459: 125020.
- [18] Wang Y P, Ni X Q, Wang M, et al. Demodulation of an optical fiber MEMS pressure sensor based on single bandpass microwave photonic filter[J]. Optics Express, 2017, 25(2): 644-653.
- [19] 赵士元, 崔继文, 陈勳勳. 光纤形状传感技术综述[J]. 光学精密工程, 2020, 28(1): 10-29.
Zhao S Y, Cui J W, Chen M M. Review on optical fiber shape sensing technology[J]. Optics and Precision Engineering, 2020, 28(1): 10-29.
- [20] 金凯, 丁莉芸, 郭会勇, 等. 超低温条件下光纤光栅温敏系数标定[J]. 光学精密工程, 2022, 30(1): 56-61.
Jin K, Ding L Y, Guo H Y, et al. Calibration of temperature-sensitivity coefficient of fiber Bragg grating at ultra-low temperature [J]. Optics and Precision Engineering, 2022, 30(1): 56-61.
- [21] 张伟. 光纤布拉格光栅应变传感系统可靠性的关键技术研究[D]. 重庆: 重庆大学, 2016.
Zhang W. Key technology for reliability of fiber Bragg grating strain sensing system[D]. Chongqing: Chongqing University, 2016.
- [22] 董新永, 赵春柳, 宁鼎, 等. 用光纤光栅的啁啾效应实现温度不敏感的弯曲传感[J]. 光子学报, 2001, 30(4): 425-428.
Dong X Y, Zhao C L, Ning D, et al. Temperature-independent bend sensor using chirp effect of fiber Bragg grating[J]. Acta Photonica Sinica, 2001, 30(4): 425-428.
- [23] 杨淑连, 何建廷, 魏芹芹, 等. 强度调制的光纤布拉格光栅磁场传感器[J]. 光学精密工程, 2014, 22(3): 597-601.
Yang S L, He J T, Wei Q Q, et al. Intensity-modulated magnetic field sensor based on optical fiber Bragg grating[J]. Optics and Precision Engineering, 2014, 22(3): 597-601.
- [24] Yang J Y, Dong X Y, Jin S Z, et al. Magnetic field sensor based on reflection spectrum measurement of fiber Bragg grating[J]. Proceedings of SPIE, 2014, 9157: 91571F.
- [25] 陈考奎, 李院峰, 周次明, 等. 基于弱光纤布拉格光栅阵列的桥梁应变测量[J]. 激光与光电子学进展, 2022, 59(7): 0706003.
Chen K K, Li Y F, Zhou C M, et al. Bridge strain measurement based on weak fiber Bragg grating array[J]. Laser & Optoelectronics Progress, 2022, 59(7): 0706003.
- [26] 殷礼鑫, 刘智超, 刘春辉. 基于 FBG 阵列的曲面结构状态感知系统[J]. 中国激光, 2021, 48(24): 2406001.
Yin L X, Liu Z C, Liu C H. Surface structure state perception system based on FBG array[J]. Chinese Journal of Lasers, 2021, 48(24): 2406001.
- [27] Shiratsuchi T, Imai T. Development of fiber Bragg grating strain sensor with temperature compensation for measurement of cryogenic structures[J]. Cryogenics, 2021, 113: 103233.
- [28] Malakzadeh A, Mansoursamaei M, Pashaie R. Simultaneous measurement of temperature and strain based on peak power changes and wavelength shift using only one uniform fiber Bragg grating[J]. Optical and Quantum Electronics, 2021, 53(5): 208.
- [29] Liu Z, Gu X Y, Wu C Y, et al. Studies on the validity of strain sensors for pavement monitoring: a case study for a fiber Bragg grating sensor and resistive sensor[J]. Construction and Building Materials, 2022, 321: 126085.
- [30] Sun L, Li C, Zhang C W, et al. The strain transfer mechanism of fiber Bragg grating sensor for extra large strain monitoring[J]. Sensors, 2019, 19(8): 1851.
- [31] Tan R S, Chen C, Zheng Y Q, et al. High-precision calibration method for fiber Bragg grating strain sensing based on an optical lever[J]. Optical Fiber Technology, 2021, 61: 102392.
- [32] Tu K, Xie Z W, Zeng W L, et al. High temperature accurate monitoring based on phase-shifting grating and photoelectric oscillation[J]. IEEE Photonics Technology Letters, 2021, 33(21): 1169-1172.
- [33] 陈梓泳, 何俊, 徐锡镇, 等. 飞秒激光逐点法制备光纤布拉格光栅高温传感器阵列[J]. 光学学报, 2021, 41(13): 1306002.
Chen Z Y, He J, Xu X Z, et al. High-temperature sensor array based on fiber Bragg gratings fabricated by femtosecond laser point-by-point method[J]. Acta Optica Sinica, 2021, 41(13): 1306002.
- [34] Peng J, Jia S H, Yu H Q, et al. Design and experiment of FBG sensors for temperature monitoring on external electrode of lithium-ion batteries[J]. IEEE Sensors Journal, 2021, 21(4): 4628-4634.
- [35] 杨颂, 刘延超, 雷威道, 等. 光纤传感技术在超导磁体状态监测中的应用研究[J]. 激光与光电子学进展, 2021, 58(11): 1106008.
Yang S, Liu Y C, Lei X D, et al. Application of optical fiber sensing technology in state monitoring of superconducting magnet [J]. Laser & Optoelectronics Progress, 2021, 58(11): 1106008.
- [36] Schenato L, Aguilar-López J P, Galtarossa A, et al. A rugged FBG-based pressure sensor for water level monitoring in dikes[J]. IEEE Sensors Journal, 2021, 21(12): 13263-13271.
- [37] Rosolem J B, Penze R S, Florida C, et al. Dynamic effects of temperature on FBG pressure sensors used in combustion engines [J]. IEEE Sensors Journal, 2021, 21(3): 3020-3027.
- [38] Rente B, Fabian M, Vidakovic M, et al. A fiber Bragg grating (FBG)-based sensor system for anaerobic biodigester humidity monitoring[J]. IEEE Sensors Journal, 2021, 21(2): 1540-1547.
- [39] Guo J Y, Shi B, Sun M Y, et al. Characterization of an ORMOCER[®]-coated FBG sensor for relative humidity sensing[J]. Measurement, 2021, 171: 108851.
- [40] Duan Z H, Jiang Y D, Tai H L. Recent advances in humidity sensors for human body related humidity detection[J]. Journal of Materials Chemistry C, 2021, 9(42): 14963-14980.
- [41] Kaur G, Kaler R S. Investigate the optical FBG sensor to monitor displacement and vibration in civil structure[J]. Optical and Quantum Electronics, 2022, 54(2): 121.
- [42] Li T L, Guo J X, Tan Y G, et al. Recent advances and tendency in fiber Bragg grating-based vibration sensor: a review[J]. IEEE Sensors Journal, 2020, 20(20): 12074-12087.
- [43] Yu Y, Liu B, Xia F. Design optimization of sensitivity-enhanced structure for fiber Bragg grating acoustic emission sensor based on additive manufacturing[J]. Sensors, 2022, 22(2): 416.
- [44] Liu B, Yu Y, Xia F, et al. Design of a novel fiber grating acoustic emission sensor based on coupling cone structure[J]. Measurement Science and Technology, 2022, 33(9): 095113.

- [45] Nadeem M D, Raghuvanshi S K, Kumar S. Recent advancement of phase shifted fiber Bragg grating sensor for ultrasonic wave application: a review[J]. *IEEE Sensors Journal*, 2022, 22(8): 7463-7474.
- [46] Chen X L, Wu S N, Lin H G, et al. Optical fiber sensor with stable operating point for AC magnetic field measurement[J]. *Applied Sciences*, 2022, 12(14): 7049.
- [47] Zhou M H, Zhao Y C, Wang G S, et al. Simultaneous AC and DC measurement based on an FBG-magnetostrictive fiber sensor [J]. *Applied Optics*, 2021, 60(24): 7131-7135.
- [48] 董富宁, 杨庆, 罗曼丹, 等. 一种基于磁致伸缩效应和光纤光栅的电流传感器[J]. *光学学报*, 2022, 42(8): 0806001.
Dong F N, Yang Q, Luo M D, et al. Current sensor based on magnetostriction and fiber Bragg grating[J]. *Acta Optica Sinica*, 2022, 42(8): 0806001.
- [49] Song L, Fang F Z, Zhao J B. Study on viscosity measurement using fiber Bragg grating micro-vibration[J]. *Measurement Science and Technology*, 2013, 24(1): 015301.
- [50] Cheng Z W, Zhao Y H, Zhang J H, et al. Generalized modular spectrometers combining a compact nanobeam microcavity and computational reconstruction[J]. *ACS Photonics*, 2022, 9(1): 74-81.
- [51] Bodendorfer T, Muller M S, Hirth F, et al. Comparison of different peak detection algorithms with regards to spectrometric fiber Bragg grating interrogation systems[C]//2009 International Symposium on Optomechatronic Technologies, September 21-23, 2009, Istanbul, Turkey. New York: IEEE Press, 2009: 122-126.
- [52] Ezbiri A, Kanellopoulos S E, Handerek V A. High resolution instrumentation system for fibre-Bragg grating aerospace sensors [J]. *Optics Communications*, 1998, 150(1/2/3/4/5/6): 43-48.
- [53] Gong J M, MacAlpine J M K, Chan C C, et al. A novel wavelength detection technique for fiber Bragg grating sensors[J]. *IEEE Photonics Technology Letters*, 2002, 14(5): 678-680.
- [54] Caucheteur C, Chah K, Lhomme F, et al. Autocorrelation demodulation technique for fiber Bragg grating sensor[J]. *IEEE Photonics Technology Letters*, 2004, 16(10): 2320-2322.
- [55] Huang C, Jing W, Liu K, et al. Demodulation of fiber Bragg grating sensor using cross-correlation algorithm[J]. *IEEE Photonics Technology Letters*, 2007, 19(9): 707-709.
- [56] Negri L, Nied A, Kalinowski H, et al. Benchmark for peak detection algorithms in fiber Bragg grating interrogation and a new neural network for its performance improvement[J]. *Sensors*, 2011, 11(4): 3466-3482.
- [57] Yang Y, Wu J Y, Wang M H, et al. Fast demodulation of fiber Bragg grating wavelength from low-resolution spectral measurements using buneman frequency estimation[J]. *Journal of Lightwave Technology*, 2020, 38(18): 5142-5148.
- [58] 张利伟, 谭中伟, 丁志超, 等. 基于光纤光栅振动传感的快速检测系统[J]. *量子光学学报*, 2020, 26(3): 250-257.
Zhang L W, Tan Z W, Ding Z C, et al. Fast detection system based on FBG vibration sensor[J]. *Journal of Quantum Optics*, 2020, 26(3): 250-257.
- [59] 李佳, 刘锋, 李红, 等. 超声脉冲导入光纤光栅的动态光谱特性研究[J]. *激光与红外*, 2020, 50(12): 1492-1497.
Li J, Liu F, Li H, et al. Study on dynamic spectral characteristics of ultrasonic pulse into fiber Bragg grating[J]. *Laser & Infrared*, 2020, 50(12): 1492-1497.
- [60] 李政颖, 周磊, 孙文丰, 等. 基于色散效应的光纤光栅高速高精度解调方法研究[J]. *物理学报*, 2017, 66(1): 014206.
Li Z Y, Zhou L, Sun W F, et al. High speed and high precision demodulation method of fiber grating based on dispersion effect[J]. *Acta Physica Sinica*, 2017, 66(1): 014206.
- [61] Fu H Y, Liu H L, Dong X, et al. High-speed fibre Bragg grating sensor interrogation using dispersion-compensation fibre[J]. *Electronics Letters*, 2008, 44(10): 618-619.
- [62] Li Z M, Zhou L, Sun W F. A novel method for the high-speed demodulation of FBG sensor arrays[C/OL]. *AIP Conference Proceedings*, 2017, 1834: 020021. <https://doi.org/10.1063/1.4981560>.
- [63] Chitchebakov A A, Swart P L. Chirped fiber-optic Bragg grating interrogator in a multiplexed Bragg grating sensor configuration[J]. *Journal of Lightwave Technology*, 2004, 22(6): 1543-1547.
- [64] Sun Q Z, Liu D M, Liu H R, et al. Chirped fiber Bragg grating sensor based on phase delay[J]. *Proceedings of SPIE*, 2007, 6781: 67812K.
- [65] Liu J X, Lu P, Mihailov S J, et al. Real-time random grating sensor array for quasi-distributed sensing based on wavelength-to-time mapping and time-division multiplexing[J]. *Optics Letters*, 2019, 44(2): 379-382.
- [66] 李志全, 曹平, 任晓丽, 等. 啁啾光栅解调的准分布式光纤 Bragg 光栅传感器[J]. *光电子·激光*, 2011, 22(4): 491-494.
Li Z Q, Cao P, Ren X L, et al. Quasi-distributed fiber Bragg grating sensor using the demodulation of chirped grating[J]. *Journal of Optoelectronics·Laser*, 2011, 22(4): 491-494.
- [67] 刘波, 童峥嵘, 曾剑, 等. 一种利用啁啾光栅反射滤波的光纤光栅传感解调方法[J]. *光子学报*, 2004, 33(1): 57-60.
Liu B, Tong Z R, Zeng J, et al. A demodulation method based on chirp grating reflective filter in fiber Bragg grating sensing system [J]. *Acta Photonica Sinica*, 2004, 33(1): 57-60.
- [68] 秦文婕. 光纤布拉格光栅传感性能提升的信号处理方法研究[D]. 北京: 华北电力大学, 2021.
Qin W J. Research on signal processing methods for improving fiber Bragg grating sensing performance[D]. Beijing: North China Electric Power University, 2021.
- [69] 吴晶, 吴哈平, 黄俊斌, 等. 光纤光栅传感信号解调技术研究进展[J]. *中国光学*, 2014, 7(4): 519-531.
Wu J, Wu H P, Huang J B, et al. Research progress in signal demodulation technology of fiber Bragg grating sensors[J]. *Chinese Optics*, 2014, 7(4): 519-531.
- [70] 侯亚荣. 高速光纤光栅解调系统的研究与实现[D]. 武汉: 武汉理工大学, 2019.
Hou Y R. Research and implementation of high speed fiber Bragg grating demodulation system[D]. Wuhan: Wuhan University of Technology, 2019.
- [71] 李政颖, 周祖德, 童杏林, 等. 高速大容量光纤光栅解调仪的研究[J]. *光学学报*, 2012, 32(3): 0306007.
Li Z Y, Zhou Z D, Tong X L, et al. Research of high-speed large-capacity fiber Bragg grating demodulator[J]. *Acta Optica Sinica*, 2012, 32(3): 0306007.
- [72] 刘铁根, 江俊峰, 刘琨. 分立式光纤传感技术与系统[M]. 北京: 电子工业出版社, 2012.
Liu T G, Jiang J F, Liu K. Discrete optical fiber sensing technology and systems[M]. Beijing: Publishing House of Electronics Industry, 2012.
- [73] Ball G A, Morey W W, Cheo P K. Fiber laser source/analyzer for Bragg grating sensor array interrogation[J]. *Journal of Lightwave Technology*, 1994, 12(4): 700-703.
- [74] 郭峻. 基于可调谐激光器的光纤布拉格光栅传感技术研究[D]. 哈尔滨: 哈尔滨工业大学, 2016.
Guo J. Research on fiber Bragg gratings sensing based on tunable laser[D]. Harbin: Harbin Institute of Technology, 2016.
- [75] Yao Y Q, Li Z Y, Wang Y M, et al. Performance optimization design for a high-speed weak FBG interrogation system based on DFB laser[J]. *Sensors*, 2017, 17(7): 1472.
- [76] 刘泉, 王一鸣, 刘司琪, 等. 一种基于分布式反馈激光器的 FBG 高速解调系统[J]. *光电子·激光*, 2015, 26(8): 1473-1478.
Liu Q, Wang Y M, Liu S Q, et al. A high-speed FBG interrogation system based on DFB laser[J]. *Journal of Optoelectronics·Laser*, 2015, 26(8): 1473-1478.
- [77] Huber R, Wojtkowski M, Fujimoto J G. Fourier domain mode locking (FDML): a new laser operating regime and applications for optical coherence tomography[J]. *Optics Express*, 2006, 14(8): 3225-3237.
- [78] Jung E J, Kim C S, Jeong M Y, et al. Characterization of FBG

- sensor interrogation based on a FDML wavelength swept laser[J]. *Optics Express*, 2008, 16(21): 16552-16560.
- [79] Yamaguchi T, Shinoda Y. Development of FBG interrogation system using wavelength sweeping of FDML laser[C]//2016 IEEE SENSORS, October 30-November 3, 2016, Orlando, FL, USA. New York: IEEE Press, 2017.
- [80] Yamaguchi T, Shinoda Y. High-speed vibration measurement by fiber Bragg gratings with Fourier domain mode locking laser[J]. *Proceedings of SPIE*, 2017, 10323: 103232I.
- [81] Yamaguchi T, Endo W, Shinoda Y. High-speed interrogation system for fiber Bragg gratings with buffered Fourier domain mode-locked laser[J]. *IEEE Sensors Journal*, 2021, 21(15): 16659-16669.
- [82] Wang C, Yao J P. Ultrafast and ultrahigh-resolution interrogation of a fiber Bragg grating sensor based on interferometric temporal spectroscopy[J]. *Journal of Lightwave Technology*, 2011, 29(19): 2927-2933.
- [83] Kim H, Song M. Fiber laser FBG sensor system by using a spectrometer demodulation[J]. *Proceedings of SPIE*, 2011, 8073: 80730B.
- [84] 张正一. 基于光谱法的光纤光栅高速高分辨率解调系统研究[D]. 重庆: 重庆大学, 2019.
- Zhang Z Y. Study on high-speed and high-resolution demodulation system of fiber grating based on spectroscopy[D]. Chongqing: Chongqing University, 2019.
- [85] 张军英, 王冰, 王伟, 等. 基于线阵扫描的FBG高温传感解调系统[J]. *激光杂志*, 2021, 42(10): 59-63.
- Zhang J Y, Wang B, Wang W, et al. FBG high temperature sensor demodulation system based on linear array scanning[J]. *Laser Journal*, 2021, 42(10): 59-63.
- [86] Ma L M, Ma C, Wang Y M, et al. High-speed distributed sensing based on ultra weak FBGs and chromatic dispersion[J]. *IEEE Photonics Technology Letters*, 2016, 28(12): 1344-1347.
- [87] Fernández M P, Bulus Rossini L A, Cruz J L, et al. High-speed and high-resolution interrogation of FBG sensors using wavelength-to-time mapping and Gaussian filters[J]. *Optics Express*, 2019, 27(25): 36815-36823.
- [88] 陈显, 余尚江, 杨吉祥, 等. 线性滤波法高速解调技术中的测量有效性研究[J]. *光学学报*, 2009, 29(1): 145-150.
- Chen X, Yu S J, Yang J X, et al. Measurement efficiency of high-speed-demodulation by linear filtering method[J]. *Acta Optica Sinica*, 2009, 29(1): 145-150.
- [89] Melle S M, Liu K, Measures R M. A passive wavelength demodulation system for guided-wave Bragg grating sensors[J]. *IEEE Photonics Technology Letters*, 1992, 4(5): 516-518.
- [90] 乔学光, 丁锋, 贾振安, 等. 基于光源滤波的高精度光纤光栅地震检波解调系统[J]. *光学学报*, 2010, 30(8): 2219-2223.
- Qiao X G, Ding F, Jia Z A, et al. High precision optical fiber Bragg grating demodulation system based on the source filtering for seismic detection[J]. *Acta Optica Sinica*, 2010, 30(8): 2219-2223.
- [91] 陈宸, 李仙丽, 丁晖. 新型波长解调技术在干涉型光纤传感器输出解调中的应用[J]. *光谱学与光谱分析*, 2017, 37(9): 2948-2953.
- Chen C, Li X L, Ding H. A novel wavelength demodulation technique for interferometric fiber optic sensor[J]. *Spectroscopy and Spectral Analysis*, 2017, 37(9): 2948-2953.
- [92] 刘波, 童峥嵘, 陈少华, 等. 一种长周期光纤光栅边缘滤波线性解调新方法[J]. *光学学报*, 2004, 24(2): 199-202.
- Liu B, Tong Z R, Chen S H, et al. A novel method of edge filter linear demodulation using long-period grating in fiber sensor system[J]. *Acta Optica Sinica*, 2004, 24(2): 199-202.
- [93] 张燕君, 王光宇, 付兴虎. 长周期光纤光栅-布拉格光纤光栅多波长解调[J]. *光电工程*, 2016, 43(8): 13-17.
- Zhang Y J, Wang G Y, Fu X H. Multiple wavelength demodulation method of long period fiber grating and fiber Bragg grating[J]. *Opto-Electronic Engineering*, 2016, 43(8): 13-17.
- [94] 陈瑞姣, 葛海波, 张杰, 等. 可调谐环形双边缘滤波FBG解调系统的设计[J]. *光通信技术*, 2015, 39(10): 24-26.
- Chen R J, Ge H B, Zhang J, et al. Design of FBG demodulation system based on tunable ring double edge filter[J]. *Optical Communication Technology*, 2015, 39(10): 24-26.
- [95] 范典, 姜德生, 梅加纯. 高速双边缘光纤光栅波长解调技术[J]. *光子学报*, 2006, 35(1): 118-121.
- Fan D, Jiang D S, Mei J C. High-speed double-edged wavelength interrogation technology for fiber Bragg grating[J]. *Acta Photonica Sinica*, 2006, 35(1): 118-121.
- [96] 姜明顺, 孟玲, 隋青美, 等. 一种新颖的双边缘滤波光纤布拉格光栅解调技术[J]. *光电子·激光*, 2011, 22(3): 355-358.
- Jiang M S, Meng L, Sui Q M, et al. A novel double-edged filter wavelength interrogation technology for FBGs[J]. *Journal of Optoelectronics·Laser*, 2011, 22(3): 355-358.
- [97] Davis M A, Kersey A D. All-fibre Bragg grating strain-sensor demodulation technique using a wavelength division coupler[J]. *Electronics Letters*, 1994, 30(1): 75-77.
- [98] Sano Y, Yoshino T. Fast optical wavelength interrogator employing arrayed waveguide grating for distributed fiber Bragg grating sensors[J]. *Journal of Lightwave Technology*, 2003, 21(1): 132-139.
- [99] Ji S K, Li K, Yuan P, et al. Design and fabrication of AWG with large bandwidth applied in FBG interrogation system[J]. *Optics & Laser Technology*, 2022, 149: 107372.
- [100] 梁有程, 江绍基, 余志强, 等. 基于非对称F-P滤波器的光纤光栅解调技术[J]. *红外与激光工程*, 2007, 36(6): 906-909.
- Liang Y C, Jiang S J, Yu Z Q, et al. Fiber Bragg grating sensor demodulation technique based on asymmetric F-P filter[J]. *Infrared and Laser Engineering*, 2007, 36(6): 906-909.
- [101] 刘睿, 葛海波, 何其睿, 等. 基于F-P腔的双边缘滤波解调系统研究[J]. *光通信研究*, 2018, 44(2): 51-54.
- Liu R, Ge H B, He Q R, et al. Research on double-edged filter demodulation system based on F-P cavity[J]. *Study on Optical Communications*, 2018, 44(2): 51-54.
- [102] Cheben P, Post E, Janz S, et al. Tilted fiber Bragg grating sensor interrogation system using a high-resolution silicon-on-insulator arrayed waveguide grating[J]. *Optics Letters*, 2008, 33(22): 2647-2649.
- [103] Tiwari U, Thyagarajan K, Shenoy M R, et al. EDF-based edge-filter interrogation scheme for FBG sensors[J]. *IEEE Sensors Journal*, 2013, 13(4): 1315-1319.
- [104] Ogawa K, Koyama S, Haseda Y, et al. Wireless, portable fiber Bragg grating interrogation system employing optical edge filter[J]. *Sensors*, 2019, 19(14): 3222.
- [105] Orr P, Niewczas P. High-speed, solid state, interferometric interrogator and multiplexer for fiber Bragg grating sensors[J]. *Journal of Lightwave Technology*, 2011, 29(22): 3387-3392.
- [106] Kouroussis G, Kinet D, Mendoza E, et al. Edge-filter technique and dominant frequency analysis for high-speed railway monitoring with fiber Bragg gratings[J]. *Smart Materials and Structures*, 2016, 25(7): 075029.
- [107] 王维, 葛海波, 李盼盼, 等. 基于双芯LPPG边缘滤波的动态解调系统[J]. *光通信技术*, 2018, 42(10): 46-48.
- Wang W, Ge H B, Li P P, et al. Dynamic demodulation system based on twin-core LPPG edge filtering[J]. *Optical Communication Technology*, 2018, 42(10): 46-48.
- [108] Ding Z C, Tan Z W, Su X X, et al. A fast interrogation system of FBG sensors based on low loss jammed-array wideband sawtooth filter[J]. *Optical Fiber Technology*, 2019, 48: 128-133.
- [109] 张婧. 基于阵列波导光栅的高频动态应变传感系统[D]. 重庆: 重庆理工大学, 2021.
- Zhang J. High frequency dynamic strain sensor system based on array waveguide grating[D]. Chongqing: Chongqing University of Technology, 2021.
- [110] 丁志超. 光纤干涉仪传感器及波长解调系统的理论与实验研究[D]. 北京: 北京交通大学, 2021.
- Ding Z C. Theoretical and experimental study on fiber interferometer sensor and wavelength interrogation system[D]. Beijing: Beijing Jiaotong University, 2021.

- [111] Wang C, Shang Y, Zhao W A, et al. Distributed acoustic sensor using broadband weak FBG array for large temperature tolerance [J]. *IEEE Sensors Journal*, 2018, 18(7): 2796-2800.
- [112] Kersey A D, Berkoff T A, Morey W W. High-resolution fibre-grating based strain sensor with interferometric wavelength-shift detection[J]. *Electronics Letters*, 1992, 28(3): 236-238.
- [113] 吴小蓉, 顾金良, 王康, 等. 基于耦合器的FBG应变解调系统[J]. *光通信技术*, 2016, 40(1): 19-21.
Wu X R, Gu J L, Wang K, et al. FBG strain demodulation system based on the coupler[J]. *Optical Communication Technology*, 2016, 40(1): 19-21.
- [114] 余有龙, 谭华耀, 鍾永康. 基于干涉解调技术的光纤光栅传感系统[J]. *光学学报*, 2001, 21(8): 987-989.
Yu Y L, Tan H Y, Zhong Y K. A fiber Bragg grating sensor system with interferometric demodulation technique[J]. *Acta Optica Sinica*, 2001, 21(8): 987-989.
- [115] Wei H M, Tao C Y, Zhu Y N, et al. Fiber Bragg grating dynamic strain sensor using an adaptive reflective semiconductor optical amplifier source[J]. *Applied Optics*, 2016, 55(10): 2752-2759.
- [116] Chung S, Kim J, Yu B A, et al. A fiber Bragg grating sensor demodulation technique using a polarization maintaining fiber loop mirror[J]. *IEEE Photonics Technology Letters*, 2001, 13(12): 1343-1345.
- [117] Zhao D H, Shu X W, Lai Y C, et al. Fiber Bragg grating sensor interrogation using chirped fiber grating-based Sagnac loop[J]. *IEEE Sensors Journal*, 2003, 3(6): 734-738.
- [118] 张锦龙, 王葵如, 余重秀, 等. 基于保偏光纤的高精度光纤光栅传感解调方案[J]. *中国激光*, 2009, 36(3): 727-731.
Zhang J L, Wang K R, Yu C X, et al. A high-precision demodulation scheme for fiber grating sensors based on polarization-maintaining fiber[J]. *Chinese Journal of Lasers*, 2009, 36(3): 727-731.
- [119] Oton C J, Tozzetti L, Pasquale F D. High-speed FBG interrogation with electro-optically tunable Sagnac loops[J]. *Journal of Lightwave Technology*, 2020, 38(16): 4513-4519.
- [120] Song M, Yin S, Ruffin P B. Fiber Bragg grating strain sensor demodulation with quadrature sampling of a Mach-Zehnder interferometer[J]. *Applied Optics*, 2000, 39(7): 1106-1111.
- [121] Mohan D K, Gaurav T, Khijwania Sunil K, et al. Design and numerical analysis of a highly sensitive ultrasonic acoustic sensor based on pi-phase-shifted fiber Bragg grating and fiber Mach-Zehnder interferometer interrogation[J]. *Metrology and Measurement Systems*, 2020, 27(2): 289-300.
- [122] Lekki J D, Adamovsky G, Floyd B. Demodulation system for fiber optic Bragg grating dynamic pressure sensing[J]. *Proceedings of SPIE*, 2001, 4328: 151-159.
- [123] 刘波. 光纤光栅传感系统的研究与实现[D]. 天津: 南开大学, 2004.
Liu B. Research and realization of fiber grating sensing networks [D]. Tianjin: Nankai University, 2004.
- [124] Cao Y P, Zhang H M, Miao Y P, et al. Simultaneous measurement of temperature and refractive index based on microfiber Bragg grating in Sagnac loop[J]. *Optical Fiber Technology*, 2019, 47: 147-151.
- [125] Huang F Q, Chen T, Si J H, et al. Fiber laser based on a fiber Bragg grating and its application in high-temperature sensing[J]. *Optics Communications*, 2019, 452: 233-237.
- [126] Ding Z C, Tan Z W. Strain and temperature discrimination based on a Sagnac interferometer with three sections of high birefringence fibers[J]. *Journal of the Optical Society of America B*, 2020, 37(2): 440-444.
- [127] Dong X Y, Shao L Y, Fu H Y, et al. Intensity-modulated fiber Bragg grating sensor system based on radio-frequency signal measurement[J]. *Optics Letters*, 2008, 33(5): 482-484.
- [128] Zhou J A, Xia L, Cheng R, et al. Radio-frequency unbalanced M-Z interferometer for wavelength interrogation of fiber Bragg grating sensors[J]. *Optics Letters*, 2016, 41(2): 313-316.
- [129] Li M, Li W Z, Yao J P, et al. Femtometer-resolution wavelength interrogation using an optoelectronic oscillator[C] // *IEEE Photonics Conference*, September 23-27, 2012, Burlingame, CA, USA. New York: IEEE Press, 2012: 298-299.
- [130] Liu K, Xia L, Zhou J A, et al. Static/dynamic strain interrogations of FBG sensor based on radio frequency unbalanced M-Z interferometer[C] // *2016 15th International Conference on Optical Communications and Networks (ICOON)*, September 24-27, 2016, Hangzhou, China. New York: IEEE Press, 2017.
- [131] Zhou L, Li Z Y, Xiang N, et al. High-speed demodulation of weak fiber Bragg gratings based on microwave photonics and chromatic dispersion[J]. *Optics Letters*, 2018, 43(11): 2430-2433.
- [132] Yao J P. Microwave photonic sensors[J]. *Journal of Lightwave Technology*, 2021, 39(12): 3626-3637.
- [133] Yao J P. Microwave photonics for high-resolution and high-speed interrogation of fiber Bragg grating sensors[J]. *Fiber and Integrated Optics*, 2015, 34(4): 204-216.
- [134] Hervás J, Fernández-Pousa C R, Barrera D, et al. An interrogation technique of FBG cascade sensors using wavelength to radio-frequency delay mapping[J]. *Journal of Lightwave Technology*, 2015, 33(11): 2222-2227.
- [135] Benitez J, Bolea M, Mora J. Demonstration of multiplexed sensor system combining low coherence interferometry and microwave photonics[J]. *Optics Express*, 2017, 25(11): 12182-12187.
- [136] 崔益峰, 汪弋平, 施青云, 等. 基于微波光子滤波器的高分辨率光纤横向负载传感器[J]. *光学学报*, 2018, 38(12): 1206004.
Cui Y F, Wang Y P, Shi Q Y, et al. High-resolution transverse load fiber sensor based on microwave photonic filter[J]. *Acta Optica Sinica*, 2018, 38(12): 1206004.
- [137] Li L W, Yi X K, Chew S X, et al. Double-pass microwave photonic sensing system based on low-coherence interferometry[J]. *Optics Letters*, 2019, 44(7): 1662-1665.
- [138] Wang L H, Fang Y J, Li S P, et al. FBG demodulation with enhanced performance based on optical fiber relative delay measurement[J]. *IEEE Photonics Technology Letters*, 2020, 32(13): 775-778.
- [139] Wang W X, Liu Y, Du X W, et al. Ultra-stable and real-time demultiplexing system of strong fiber Bragg grating sensors based on low-frequency optoelectronic oscillator[J]. *Journal of Lightwave Technology*, 2020, 38(4): 981-988.
- [140] 王文轩. 基于光电振荡器的微波光子技术在传感系统中的研究[D]. 南京: 南京大学, 2020.
Wang W X. Study of microwave photonic technology based on optoelectronic oscillator in sensing systems[D]. Nanjing: Nanjing University, 2020.
- [141] Xie T T, Xu Z W, Cai X, et al. Highly sensitive fiber Bragg grating sensing system based on a dual-loop optoelectronic oscillator with the enhanced vernier effect[J]. *Journal of Lightwave Technology*, 2022, 40(14): 4871-4877.
- [142] 邹朋. 航空齿轮箱的振动与模态分析研究[D]. 重庆: 重庆大学, 2018.
Zou P. The application of vibration and modal analysis in avionics gearbox[D]. Chongqing: Chongqing University, 2018.
- [143] 雷沫枝, 胡国安, 王月华, 等. 航空发动机离心叶轮高阶模态振动故障研究[J]. *振动与冲击*, 2019, 38(22): 244-250.
Lei M Z, Hu G A, Wang Y H, et al. High order mode vibration failure of an aero-engine centrifugal impeller[J]. *Journal of Vibration and Shock*, 2019, 38(22): 244-250.
- [144] 孟丽君, 谭跃刚, 周祖德, 等. 超声激励-光纤光栅检测技术的研究与发展[J]. *中国机械工程*, 2013, 24(7): 980-988.
Meng L J, Tan Y G, Zhou Z D, et al. Research and development of fiber Bragg gratings detection technology based on ultrasonic excitation[J]. *China Mechanical Engineering*, 2013, 24(7): 980-988.
- [145] Yao J P. Optoelectronic oscillators for high speed and high resolution optical sensing[J]. *Journal of Lightwave Technology*, 2017, 35(16): 3489-3497.

- [146] Hu C Y, Bai W. High-speed interrogation for large-scale fiber Bragg grating sensing[J]. *Sensors*, 2018, 18(2): 665.
- [147] Marin Y E, Nannipieri T, Oton C J, et al. Current status and future trends of photonic-integrated FBG interrogators[J]. *Journal of Lightwave Technology*, 2018, 36(4): 946-953.
- [148] Liang X, Xiang N, Li Z Y, et al. Precision dynamic sensing with ultra-weak fiber Bragg grating arrays by wavelength to frequency transform[J]. *Journal of Lightwave Technology*, 2019, 37(14): 3526-3531.
- [149] Wu H, Lin Q J, Zhao N, et al. A high-frequency acceleration sensor based on fiber grating[J]. *IEEE Transactions on Instrumentation and Measurement*, 2021, 70: 7003808.

Research Progress of FBG Sensing Signal Demodulation Technology for High-Speed Dynamic Measurement

Liu Xianming^{1,2*}, Ren Yilin^{1,2}, Zhou Feng^{1,2}, Lei Xiaohua^{1,2}, Zhang Peng^{1,2}

¹Key Laboratory of Optoelectronic Technology and Systems, Ministry of Education, Chongqing University, Chongqing 400044, China;

²College of Optoelectronic Engineering, Chongqing University, Chongqing 400044, China

Abstract

Significance Fiber Bragg grating (FBG) is advantageous owing to its compact size, light weight, anti-electromagnetic interference, high-temperature resistance, and series multiplexing, and it is increasingly adopted in several fields such as aerospace, petrochemical industry, national defense, and military. The measurement and analysis of FBG reflection or transmission spectra yield the magnitude of the physical parameter to be measured (Fig. 1). Extracting characteristic information from FBG spectral signals, i.e. FBG signal demodulation, is the basis for FBG sensing measurement applications. Most of the current FBG sensing-based systems measure at frequency below 1 kHz and are mainly used in the measurement of slowly changing physical quantities such as temperature and strain. For scenarios requiring high-speed dynamic measurements, such as high-speed vibration and explosive shock, the signal demodulation scheme based on FBG sensing must satisfy the measurement speed requirements for effective application. Depending on the measurement parameters, the FBG signal high-speed demodulation methods can be divided into four categories: spectral, optical-intensity, phase, and microwave spectrum analyses (Fig. 2).

The spectral analysis method (Section 3) relies on the full FBG spectrum for measurement analysis, which can be achieved via dispersive and scanning spectroscopies. Spectral measurement based on the principle of dispersion (Section 3.1) can be divided into spatial- and time-dispersion methods. Spectral measurement using the principle of spatial dispersion is the main method for FBG demodulation. The test speed depends on the scanning speed of the spectral acquisition device such as the charged-couple device (CCD). Spectral measurement systems using the principle of time dispersion require ultra-high-speed acquisition equipment. To obtain sufficient time delay, the length of the dispersion element is quite long. Hence, reducing the size of the dispersion element and guaranteeing a sufficient amount of dispersion is the key to its application. Using tunable light sources such as distributed Bragg reflector (DBR), distributed-feedback laser (DFB), Fourier domain mode-locked laser (FDML), and high-speed detectors can also obtain FBG characteristic spectrum, i.e., scanning spectroscopy (Section 3.2). The scanning speed of the tunable light source is the main factor that determines the testing speed of the system. Light intensity analysis (Section 4) can be achieved by single- (Section 4.1) or double-edge filtering (Section 4.2). The corresponding measurement system has no mechanical structure, and the measurement speed can easily reach the megahertz level. Its measurement range, sensitivity, and linearity are determined by the performance of the filter device. Presently, the optical filter components available are long-period fiber grating (LPFG), array waveguide grating (AWG), Fabry-Perot (FP) cavity, *etc.* The phase analysis method (Section 5) demodulates the interference signal by measuring its phase. Common systems include the Mach-Zehnder (Section 5.1), Michelson (Section 5.2), and Sagnac (Section 5.3) interference structures. Although precision is high, the demodulation range is small, and demodulation speed of several hundred kilohertz can be achieved. Microwave spectrum analysis (Section 6) converts optical domain signals into microwave frequency domain for signal analysis. The system structure of this method is very flexible, the sensitivity is high, and the speed generally depends on the back-end data acquisition system. Each of these demodulation methods has its own advantages and disadvantages. The actual application needs to be selected according to different requirements. For the measurement of vibration and dynamic strain of large structures such as bridges and rails, the application environment is relatively stable, and the measurement speed and range requirements may be relatively low. Multi-point monitoring with distributed sensing can improve efficiency and cost-effectiveness. Long-term use has high requirements for measurement accuracy, system stability, and actual data output. Scanning spectrum measurement methods or microwave spectrum analysis methods are optimal choices. However, for the instantaneous monitoring of the shock power of the explosion shock wave and the target load response, the single-point and high-speed acquisition methods are more suitable. Such transient measurements require high speed and range, the measurement time is short and signal can be collected first and then processed. Accordingly, the light intensity analysis method can be adopted. We can maximize the unique advantages of various demodulation methods and achieve efficient and accurate measurements only by selecting different high-speed demodulation

methods according to different scenarios.

Progress The spatial dispersion method is relatively mature. The Wasatch Cobra-S 800 spectrometer has a sampling rate of 250 kHz (Table 1). The measurement frequency of the systems based on the principle of time dispersion can up to 264 MHz (Table 1). In the scanning spectrometry measurement method, Tatsuya Yamaguchi *et al.* achieved a measurement frequency of 202.8 kHz driven by a conventional FDML laser with a scanning frequency of 50.7 kHz by processing the light source (Table 1). In the light intensity analysis method, Ding Z C *et al.* of Beijing Jiaotong University employed a cross-Sagnac loop as an edge filter to achieve a demodulation frequency of 200 kHz (Table 2). In the phase analysis method, Oton C *et al.* of the University of Florence achieved a demodulation speed of 100 kHz using an electro-optical modulator as a tunable retarder in the Sagnac loop (Table 3). In the microwave spectrum analysis method, Zhou Lei *et al.* used a cross-scan period to form a beat frequency, doubling the measurement frequency to 40 kHz. It has also been reported that the acquisition speed of this method can reach the megahertz level (Table 4).

Conclusions and Prospects This paper summarizes the main advantages and disadvantages of each method, the adaptation scenarios, and whether multi-grating measurement can be performed (Table 5); in addition, it sorts out some scenarios involving high-speed dynamic measurements and the corresponding high-speed demodulation methods (Fig. 24), and looks forward to the future research direction of high-speed FBG demodulation methods. First, it is important to continue to improve the FBG signal demodulation speed, which requires further improvement of the speeds of signal acquisition and processing. The methods involve increasing the rate level of light sources, line array detectors, and other devices, and optimizing the demodulation algorithms. Second, it is important to improve the accuracy and demodulation range. The spectral range and resolution of the light source need to be increased. In addition, it is important to increase the FBG demodulation capacity. While improving the speed of spectral measurement, further expanding its spectral bandwidth is the basis for the development of quasi-distributed large-capacity FBG high-speed demodulation technology.

Key words gratings; signal demodulation; fiber sensing; high-speed dynamic measurement